ESTIMATION OF HYDRAULIC PARAMETERS OF THE SHALLOW, PERCHED OHANGWENA AQUIFER (KOH-0) AND DETERMINATION OF ITS INTERACTION WITH THE DEEPER REGIONAL OHANGWENA AQUIFER (KOH-1), OHANGWENA REGION, NAMIBIA

A RESEARCH THESIS

SUBMITTED IN PARTIAL FULFILMENT

OF THE REQUIREMENTS FOR THE DEGREE OF

MASTERS OF SCIENCE

OF

THE UNIVERSITY OF NAMIBIA

BY

ASTERIA LETUVENE ANANIAS

200716824

November 2015

Main Supervisor: Dr. H. Wanke

Abstract

The Ohangwena Multi-Layered Aquifer (KOH) is one of the six Aquifer Systems found in the Cuvelai-Etosha Basin, Namibia. The aquifer system is multi layered, consisting of a shallow perched Ohangwena 0 aquifer (KOH-0), semi-confined Ohangwena I aquifer (KOH-1), and confined Ohangwena II aquifer (KOH-2). Currently, a large portion of the population in the study area rely on water from KOH-0 by means of hand-dug wells. The occurrence and potential of this perched aquifer is not fully understood. This fact motivates the characterization of the aquifer properties, to enable more thoughtful management of the resource. The study evaluates the hydraulic properties of KOH-0 and determine its connection to KOH-1. The methods used in this study included soil sampling, analysis for grain size distribution and review of existing borehole lithology logs. Examination of existing borehole lithology logs indicate that the perched KOH-0 is contained in the Kalahari sand layer from the surface up to 30 m depths, underlain by a multi-layered semi-confining layer with alternating silty sands, clays and calcrete. Based on the documented textures and standard hydraulic conductivity tables, KOH-0 has hydraulic conductivities from 1.20E-04 to 2.83E-04 m/sec and the multi-layered aquitard below, from 3.17E-9 to 1.90E-4 m/sec. Grain size analyses of the aquifer material show that the material consist of fine to course grained sand indicating a hydraulic conductivity that spans between 10^{-6} and 10^{-4} m/sec, a porosity between 0.49 and 16.25% and a coefficient of uniformity between 0.369 and 25. Potentially an amount between 2.01E-03 and 5.02E-03 m^3/day, may flow from the perched KOH-0 into the unconfined KOH-1 per square meter of aquitard. The

estimated amount of horizontal flow through KOH-1 is much higher than this, ranging relatively between 690 m^3/day (at minimum hydraulic gradient) and 6700 m^3/day (maximum hydraulic gradient). The results have shown that KOH-0 is hydraulically connected to KOH-1, especially in the northern part of the study area with higher hydraulic gradients where most hand dug wells occur and groundwater is younger. This will aid future groundwater development and utilization in the study area.

Table of Contents

List of Figures

List of Tables

List of Abbreviations

BGR	German Federal Institute of Geosciences and Natural Resources
BIWAC	Bittner Water Consult
CEB	Cuvelai-Etosha Basin
DWAF	Department of Water Affairs and Forestry
fs, ms, cs	fine sand, medium sand, course sand
K_f, K	hydraulic conductivity
KOH	Kalahari Ohangwena Multi-Layered Aquifer
m/day	meter per day
m^2/day	meter squared per day
m/sec	meter per second
m^3/sec	m^3/sec
Ma	Million years
med	medium
mm	milli meter
MAWF	Ministry of Agriculture Water and Forestry
RWL	Rest Water Level

T	Transmissivity
Q	total groundwater flow

Acknowledgement

First and foremost, I am immensely grateful for the opportunity to take part in this research project, an opportunity afforded to me by the Grace of our Heavenly Father.

My heartfelt appreciation goes to the Southern African Science Service Centre for Climate Change and Adaptive Land Management (SASSCAL) for providing funds for projects aimed at improving and understanding groundwater and many other projects. This study would not have been possible without your generous sponsorship.

The successful completion of this study has been made possible through the practical and professional support and advice of several people and departments:

- Dr. Heike Wanke (main supervisor), a special thanks goes to you for initiating and procuring funds for this study. Your insights and suggestions furthered my education through the successful completion of this study.

- Mr. Christoph Lohe, I am thankful to you for your supervision and the various discussions we had which helped me overcome some of the technical problems I encountered during the course of my study.

- Mr. Martin Quinger (Project Manager (BGR): Groundwater for the North of Namibia), I appreciate your patience, understanding and support.

- Department of Water Affairs and Forestry (Geohydrology Division), I remain indebted to you for allowing me access to your data and literature. Let's pave the future for groundwater studies in order to improve water supply in our communities.

- Josefina Hamutoko, I am profoundly thankful to you for helping me solve some of the problems I encountered with your expert advice.

- Matthias Beyer and Marcel Gaj, thank you for sharing your soil samples and laboratory analysis with me.

- Every other person who has contributed directly or indirectly to completion of my study, I will forever be thankful.

To my family and friends thank you for your patience, understanding and support

Dedication

Although only two years old, this thesis is dedicated to my little boy, Chris Tangi Imalwa. Son, all this time throughout my course work, field work and write up of my thesis, you have been my pillar of strength and motivation. I hope this thesis will serve as an inspiration to you in your future endeavors.

Love, Mom.

Declaration

I, Asteria L. Ananias, declare hereby that this study is a true reflection of my own research, and that this work, or part thereof has not been submitted for a degree in any other institution of higher education.

……... …….....

Asteria L. Ananias Date

1. Introduction

1.1. Orientation of the Study

Namibia is the driest country in Southern Africa and relies greatly on groundwater for water supply. In the Cuvelai-Etosha Basin (CEB), located in the north central part of Namibia, the population density is high and demand for water is increasing. Initially people were drawn to this part of the country by the accessibility of groundwater by hand dug wells. Even though a pipeline system was established to provide fresh water from the Kunene River via the Calueque Dam, today a large number of the population still continue to utilize hand dug wells for their everyday water supply although the quality of these waters is unknown and not monitored and the sustainability of the abstraction is not assessed.

The movement of groundwater through geological formations depends on the hydraulic parameters of the geological units. An understanding of the aquifer characteristics plays a significant role in the efficient development and management of groundwater resources as well as in addressing issues such as salinization and pollution to aquifers.

1.2. Problem Statement

According to Christellis et al. (2001), groundwater resources in the CEB have been used for over a century but their occurrence, magnitude and potential is still not fully understood. This is especially the case with the perched aquifer system.

Most of the previous research done in the study area have focused on the middle and deep aquifers[1] and have neglected the shallow aquifers[2]. The project "Groundwater for the North of Namibia" under the framework of the German Institute of Geosciences and Natural Resources (BGR) and the Ministry of Agriculture, Water and Forestry (MAWF) cooperation has seen to the development of a monitoring network for the deeper Aquifers in the CEB. However, the hydraulic parameters in the study area have rarely been quantified and the mechanisms controlling them are poorly understood. Also, no monitoring network has been created for the perched aquifer system.

1.3. Aims and Objectives

The primary aim of this project is to estimate the hydraulic parameters of the perched Kalahari Ohangwena 0 (KOH-0) Aquifer. To accomplish this primary aim, the project has been divided into the following four objectives:

i. establish the geological framework and spatial extent of the perched aquifer from existing drill hole data
ii. review and compile existing hydraulic parameter values for Kalahari Ohangwena I (KOH-1)
iii. estimate the hydraulic parameters of KOH-0
iv. determine if there is a connection between the perched aquifer and the underlying KOH-1

[1] Aquifers found between 60-300 m in the study area and accessed via boreholes.
[2] Aquifers accessed via hand dug wells

1.4. Thesis Outline

The first chapter gives an introduction to the project. This is followed by chapter 2, a review of the available literature concerning the project. Chapter three provides a general description of the project area including its geological and hydrogeological setting. In chapter four, the field and laboratory methods and materials used are presented. The methods used to analyze and evaluate the data will also be presented here. Chapter five will present the results obtained and their analysis. An interpretation and discussion of the results is presented under chapter six. Chapter seven provides conclusions drawn from the presented results and recommendations for further studies.

2. Literature Review

2.1. Characteristics and Features of Perched Aquifers

According to Fitts (2002), perched aquifers are zones of saturation completely surrounded by unsaturated zones (see Figure 1). These are unconfined water-bearing units within a vadose zone. Perched aquifers develop from surface water sources infiltrating through the unsaturated zone and accumulating on a layer of less permeable lithology such as clay. Perched aquifers are of limited areal extent and wells tapping them yield only temporary or small quantities of water.

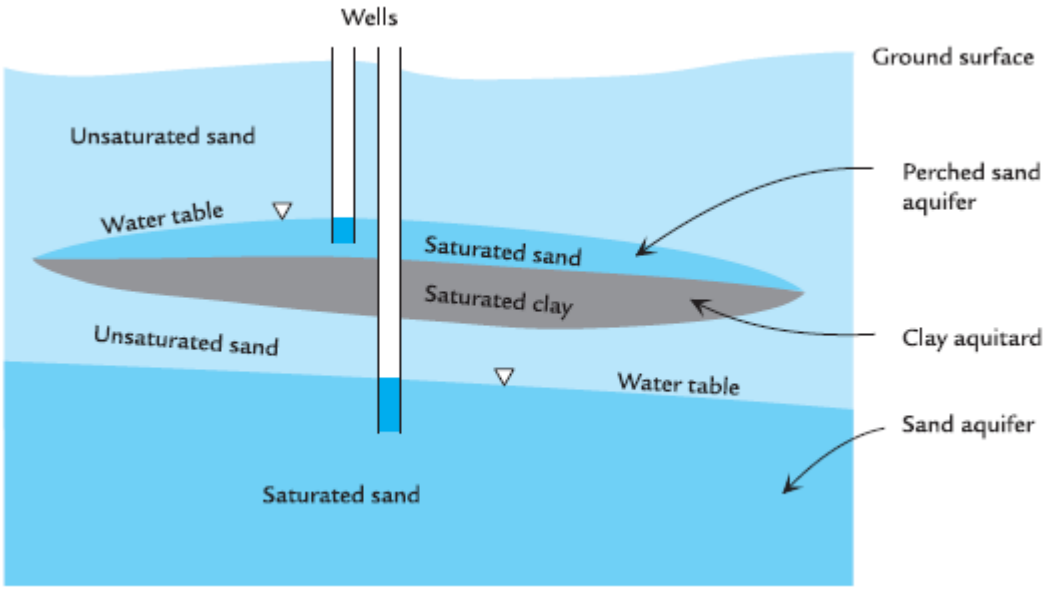

Figure 1. Schematic cross-section of a perched aquifer (Fitts, 2002).

Generally, perched water bodies are ignored or given very little importance in terms of water supply, however in areas with insufficient water supply sources, perched aquifers may be important sources. Also, perched aquifers may contribute to contaminant transport to the local aquifers.

Very limited research on perched aquifers is available with main focus on the role of these water bodies on local and regional groundwater investigations. Most studies investigated the role of perched aquifers as a groundwater migration pathway for potential contaminants, focusing on the presence or absence of contaminants in the perched units and the connectivity of these units within the groundwater system (e.g. Reichard et al., 1995, Cozarelli et al., 1999, Behera et al., 2003).

2.2. Aquifer Hydraulic Parameters

Water contained within the interconnected voids of soils and rocks is capable of moving, and the ability of a rock to store and transmit water constitutes its hydraulic properties (Hiscock, 2005). These hydraulic properties are transmissivity/permeability and storativity. The term transmissivity is used to describe the rate of groundwater flow through a cross-section of unit width and whole thickness of the aquifer, under unit hydraulic gradient. It is a product of the aquifer thickness and permeability and has a unit of meter square per day (m^2/day). The amount of water released or stored into the change in the head of aquifer normal to the surface area of the aquifer is known as the storage coefficient (storativity) or specific yield (Thangarajan, 2007) which is a non-dimensional quantity. Generally, the term storativity is used to refer to a confined aquifer and specific yield refers to an unconfined

aquifer. Permeability is a term that describes a property of the aquifer material or medium and is often referred to as the hydraulic conductivity. Permeability is expressed as the quantity of water which flows across the unit cross-section of the aquifer under unit hydraulic gradient per unit and is expressed in meter per day (m/day).

To assess the groundwater potential or evaluate the impact of pumping on the groundwater regime, it is essential to know the aquifer parameters. Aquifer hydraulic parameters can be estimated by either means of in-situ tests or by performing tests on aquifer samples brought in the laboratory (Thangarajan, 2007). The aquifer properties determined in this study are effective porosity, uniformity coefficient and hydraulic conductivity.

2.3. Effective Porosity

The porosity of a sediment is defined as the fraction of the soil's volume that is not occupied by solids (Kruseman & de Ridder, 1991; Fitts, 2002; Hiscock, 2005). In quantitative terms, porosity is given by:

$$n = \frac{V_v}{V_t},$$

where V_v is the volume of voids (air plus water) in total volume of material V_t. The porosity of a material is a dimensionless parameter in the range of $0 < n < 1$ which is sometimes expressed as a percentage. According to Hiscock (2005), the effective porosity, n_e, of a geological material relates to its transmissive capability. Effective porosity is given by:

$$n_e = \frac{V_v}{V_t}$$

,

where, V_v is the volume of voids that is interconnected and transmitting flow and V_t is the total volume of material. Effective porosity, which also refers to the spore space available for fluid flow, differs from porosity which refers to the storage capability of the material. The porosity of a soil is greatly controlled by the shape and arrangement of the grains, the degree of sorting, compaction, cementation, fracturing and solutional weathering. Generally, unconsolidated sediments such as gravels, sands, silts and clays have larger porosities than indurated, consolidated sediments such as sandstones and limestone (Hiscock, 2005).

2.4. Uniformity Coefficient

The uniformity coefficient of a material is a measure of how well or poorly sorted a material is. This parameter is obtained by taking the ratio of the grain size that is 60% finer by weight, d60, to that which is 10% finer by weight, d10. That is:

$$U = \frac{d_{60}}{d_{10}}$$

,

The uniformity coefficient is a dimensionless parameter. Generally, a material with U less than 4 is well sorted and that with U more than 6 is poorly sorted.

2.5. Hydraulic Conductivity

The values of hydraulic conductivity in soils vary within a wide range of several orders of magnitude, depending on the soil material. Materials with high hydraulic conductivity values allow water to move (transmit) easier than materials with relatively lower hydraulic conductivity. According to Stibinger (2014), hydraulic conductivity, K, is one of the principal and most important soil hydraulic parameters and it is an important factor in water transport in the soil used in all equations for groundwater flow. Hydraulic conductivity is defined in terms of volume per area time, $m^3/m^2/s$ or m/s (Fetter, 2000). This parameter (conductivity) is not always easily measured, but can be predicted using basic information and translating it into estimated of hydraulic conductivity. The expected representative values of K for soil materials of different textures are presented in Appendix B as well as a more detailed list of expected representative values of K based on the grain size distribution, degree of sorting, and silt content of unconsolidated soils.

2.6. Hydrogeological Concepts

To understand how water moves in the subsurface as well as the principles of hydraulic conductivities, knowledge of the physical properties of the material through which the water moves is required (Fitts, 2002). These physical properties as well as the basic physical laws are presented here.

2.4.1. Darcy's Law (Darcy, 1856)

In most groundwater investigations, questions arise about how much water is moving in the subsurface and how fast it is moving. The answers to these questions are based on groundwater flow analyses, which in turn are based on some straight forward physical principles that govern subsurface flow (Fitts, 2002). The flow of groundwater depends on the hydraulic gradient and hydraulic conductivity of the material through which it is flowing (Hiscock, 2005). This was determined by French engineer Henry Darcy in 1856 through many experiments with a specific soil (Fitts, 2002). The relationship between groundwater flow, hydraulic gradient and hydraulic conductivity is therefore described by Darcy's law for one-dimensional flow. Darcy's law also forms the basis for many useful hand calculations and computer simulations that can be made to analyze groundwater flow and can be written as:

$$v = -K\frac{dh}{dl}$$

where $v = \frac{Q}{A}$ which is the specific discharge, also known as the Darcy flux (Darcy velocity), Q is the volume rate of flow, A is the cross sectional area normal to the flow direction, $\Delta h = h_2 - h_1$, which is the head loss, Δl is the distance between the two points where the hydraulic heads are measured, $\frac{dh}{dl}$ is the hydraulic gradient and K is the constant of proportionality known as the hydraulic conductivity.

Alternatively, Darcy's law can be described as:

$$Q = -K\frac{dh}{dl}A$$

where Q [m/s^3] is the volume rate of flow through cross sectional area A [m^2], h [m] is the hydraulic head, and l [m] is the vertical distance in the soil. The coefficient of proportionality, K [m] is called the hydraulic conductivity which determines the ability of the soil fluid to flow through the soil matrix system under a specified hydraulic gradient.

2.4.2. Soil Properties

Hydraulic conductivity varies in different soils. Generally, course-grained soils have high values of hydraulic conductivity, while fine-grained silts and clays have low values (Hiscock, 2005).

2.4.2.1. Grain Size

Hydraulic conductivity is related to the grain-size distribution of granular porous material (Freeze & Cherry, 1979). This is because the distribution of grain sizes determines how much pore space is available to hold water and how easily water is transmitted through the material (Fitts, 2002). A sorted soil with large grains has a high hydraulic conductivity as compared to one which contains a mixture of grain sizes. The more multi graded a soil is, the lower the pore space and the lower the hydraulic conductivity.

2.4.2.2. Degree of Sorting

The porosity of a material is also controlled by the degree of sorting. If a sediment contains a mixture of grain sizes, the porosity will be lowered (Fetter, 2001). Well sorted unconsolidated materials such as uniform sands tend to have high porosities and high hydraulic conductivity values than poorly sorted materials with smaller particles packed between larger particles.

2.4.2.3. Degree of Compaction

Soil porosity greatly depends on the degree of compaction. The degree of compaction is defined is a comparison between dry density of a soil and the maximum dry density when the soil is compacted/dried in a laboratory.

2.4.2.4. Grain Shape

The shape of the grains is also one of the properties that affect the hydrogeological conductivity of a material (Hiscock, 2005 and Fetter 2001). The shapes of grains generally range between well-rounded to very irregular, depending on the transport mechanisms that led to their deposition. Different shapes of grains in a material create different ways for water to move through.

2.5. Measuring Hydraulic Conductivity

Hydraulic conductivity can be estimated through the analysis of particle size distribution of the sediments of interest using empirical equations. This is generally done by relating size properties of the sediment to its hydraulic conductivity.

Numerous researchers have studied the relationship between hydraulic conductivity and grain size distribution and have formulated several formulae based on experimental work done. In 1927, Kozeny proposed a formula which was later modified by Carman (1937, 1956) to become the Kozeny-Carman equation. Also, Hazen (1892), Shepherd (1989), Alyamani and Peck (1964) made attempts to develop formulae for the relationship between hydraulic conductivity and grain size distribution. The applicability of the formulae however depends on the type of soil for which the hydraulic conductivity is being estimated.

Vukovic and Soro (1992) summarized several empirical methods from former studies and presented a general formula:

$$K = \frac{g}{\nu} C f(n) d_e^2$$

where K = hydraulic conductivity; g = acceleration due to gravity; v = kinematic viscosity and de = effective grain diameter. The dynamic viscosity (μ) and fluid density (ρ) are related as follows:

$$\nu = \frac{\mu}{\rho}$$

C, f(n) and de depend on the different methods used in grain size analysis. Vukovic and Sol (1992) state that porosity (n) may be derived from the empirical relationship:

$$n = 0.255(1 + 0.83^{U})$$

where U is the coefficient of grain uniformity given by:

$$U = \frac{d_{60}}{d_{10}}$$

In the above formula d_{60} and d_{10} represent the grain diameter in mm for which 60% and 10% of the sample are finer than. The table below shows the representation of the general formula by different researchers based on their studies.

Table 1. Formulae for determination of hydraulic conductivity form grain size distribution

Researcher	**formula**	**Description**
Hazen	$K = \frac{g}{\nu} 6 * 10^{-4}[1 + 10(n - 0.26)]d_{10}^2$	Generally for uniformly graded sand. Can also be used for fine sand to gravel if U < 5 and de = 0.1 – 3 mm.
Kozeny - Carman	$K = \frac{g}{\nu} 8.3 * 10^{-3}[\frac{n^3}{(1-n)^2}]d_{10}^2$	Not appropriate for clayey or soils with de above 3 mm.

Researcher	formula	Description
Beyer	$K = \frac{g}{\nu} 6 * 10^{-4} log \frac{500}{U} d_{10}^2$	Does not consider porosity. Used for materials with heterogeneous distributions and poorly sorted grains with U = 1 – 20 and de = 0.06 – 0.6 mm.
Slitcher	$K = \frac{g}{\nu} 1 * 10^{-2} n^{3.287} d_{10}^2$	For grain sizes between 0.01 and 5 mm
Alyamani and Sen	$K = 1300\,[I_o + 0.025(d_{50} - d_{10})]^2$	I_o = intercept in mm of d_{50} and d_{10} with grain-size axis. d_{10} is the effective grain diameter and d_{50} is the median grain diameter. The equation depends on grain size analysis and also considers sorting characteristics.

2.6. Previous Work in the Study Area

In order to characterize the Ohangwena Aquifer System, Lohe et al., (2013) reviewed and interpreted existing geological information and information from recent drilling campaigns to gain more insight on the development of the sediments in Central-Northern Namibia.

From this investigation, the sediments in the Ohangwena region is described in detail and the spatial distribution of groundwater bearing layers are identified in terms of texture. Below is a description of the perched aquifer, based on the findings by Lohe et al (2013).

The Perched Aquifer consists of aeolian sheet sands that underlie the natural, broad-leaf forest area east of 16° 10’ E (grey shaded area in Figure 2). Also, in the far eastern part of the area where the broad-leaf forest becomes patchy, aeolian sand of the aquifer is still present in the intervening areas but the vegetation consists of small treeless grassy patches interspersed with acacia thorn forest in which only a few broad-leaf trees are present.

The study also found the aquifer sands to be largely fine to medium grained, with only very minor silt. Sorting is reasonably good and grains are mainly well rounded. For the most part, the aquifer has been found to be less than 10 m thick but thicknesses are variable and this sand can be absent in certain boreholes (WW 200484) or only 1-3 m in thickness. However, two areas where several boreholes have an aquifer thickness of more than 10 m are highlighted in figure 8 for the Perched Aquifer but even in these, the thickness varies from 6 to 25 m. Lohe et al., (2013) explains that this must have been an area where old, hand-dug wells were identified as having rather abundant good water. The upper 2 to 4 m of the aquifer is generally brown or light brown in colour, rarely light or dark grey. In a few boreholes, the first meter below the brown colour is red or orange in colour. The colour of the underlying part is white, off white or very light yellow.

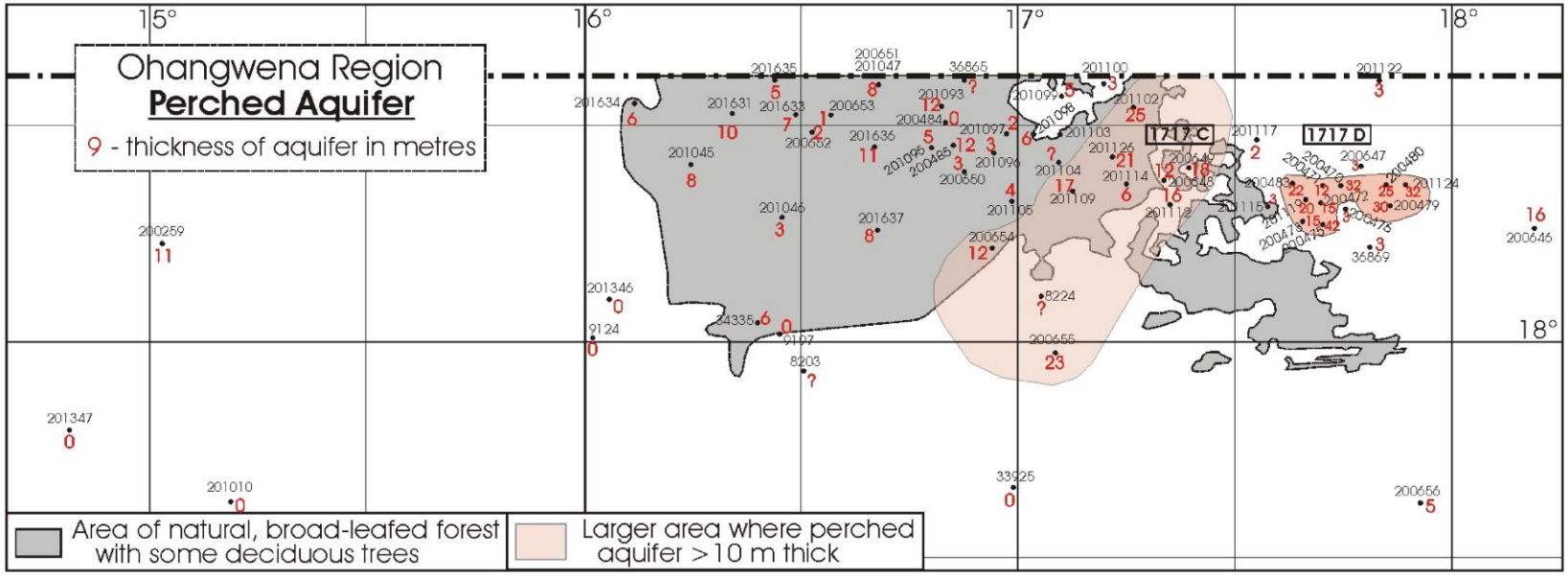

Figure 2. Thickness of perched aquifer in the Ohngwena region based on texture (Lohe et al., 2013).

Several small surveys that resulted in the determination of hydrochemical parameters such as TDS, Fluoride, Boron, Arsenic and E. coli bacteria have been conducted on the shallow aquifers by various researchers such as Amutenya (2011), Wurdac (2008) and Petrus (2012) with the use of hand dug wells. However, Hamutoko (2013) performed an assessment of the groundwater vulnerability of KOH-0 and KOH-1 using the DRASTIC and BTU method. As part of the assessment, hydraulic conductivity values were determined from grain size analysis of soils collected from various hydrotopes in the study area. Grain size analysis estimated hydraulic conductivities values for KOH-0 in the range of 5.98E-05 m/day to 3.35E-04 m/day.

Most of the research carried out in the study area focused on KOH-1 and KOH-2. Ananias (2012) evaluated various constant discharge, step-drawdown and recovery test data for KOH-1 and KOH-2 to determine the aquifer transmissivity values using the aquifer test analysis software called Aqtesolv. The transmissivity values for KOH-1 have been found to range between 0.43 and 104 m^2/day while those of KOH-2 range between 1.93 and 30.22 m^2/day. van Wyk (2009) analyzed step drawdown test data from the Rural Water Supply Drilling Program by the Department of Water Affairs and Forestry (DWAF) and Bittner Water Consult (BIWAC). The transmissivity values for KOH-1 were found to increase from west to east with values ranging between 3 and 137 m^2/day.

3. Description of the Study Area

3.1. Location

The study area is located in the Ohangwena Region within the Cuvelai-Etosha Basin, a semi-arid sedimentary basin located in the central part of Northern Namibia. The basin stretches across four administrative regions, namely Ohangwena, Omusati, Oshana and Omusati. The basin is further subdivided into four sub-basins namely Olushandja, Iishana, Niipele and Tsumeb (see figure 3).

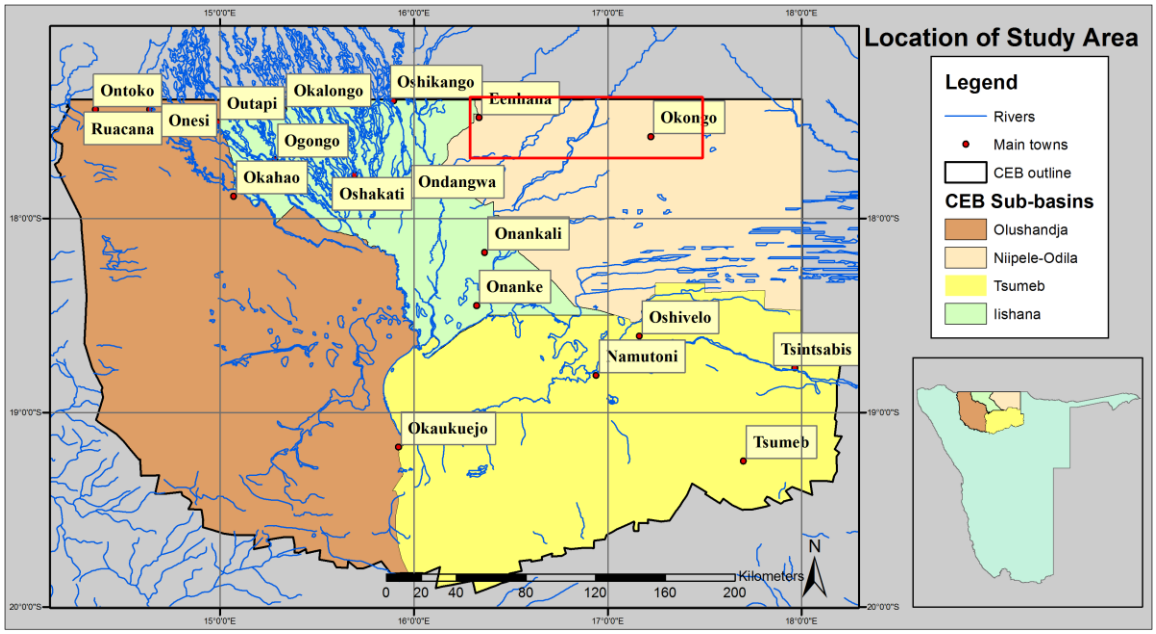

Figure 3. Location of study area.

This study is carried out in the Niipele sub-basin which is located across the Ohangwena and Oshikoto Regions. The Niipele sub-basin constitutes the Okongo constituency and

larger parts of the Epembe, Eenhana, Okankolo and Omundaungilo constituencies of the eastern part of the Ohangwena region and the northern part of the Oshikoto region. Figure 2 below shows the geographical location of the study area.

3.2. Climate

The climate around the CEB is considered to be semi-arid, with annual rainfalls low in the west and high in the east and high annual temperatures resulting in high annual evaporation. The mean annual rainfall values, as seen in Figure 4, range between 250 mm/a in the south-western part of the CEB and 600 mm/a in the area around Tsumeb (Christelis et al., 2011). 90% of the annual precipitation has been observed to occur during the period of October to March (max in February) with rainfall variability ranging between 25-40% (Bittner, 2006 after Mendelsohn et al., 2000).

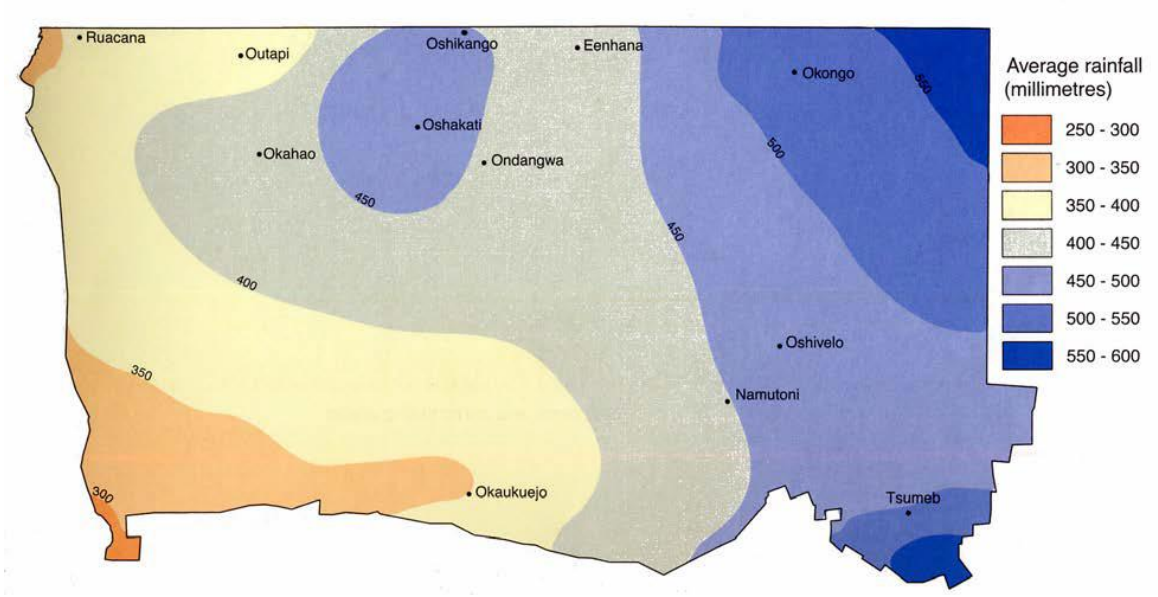

Figure 4. Mean annual rainfall across north-central Namibia (Bittner, 2006 after Mendelsohn et al., 2000).

The mean monthly values of temperatures have been recorded to be about 17^{o}C in June and about 25^{o}C from October to December. During summer, the maximum temperature ranges between 30 and 33^{o}C and decreases during winter to as low as 27^{o}C.

Humidity values are relatively low, with a range between 50% in March and 17% in September. Groundwater temperatures of about 25^{o}C are encountered in the area.

With the high evaporation rates, most pans and ephemeral rivers dry up which results in precipitation of salts and an increased salinity of shallow aquifers in particular the waterlogged areas and areas comprising of low permeable lithologies (Bittner, 2006).

3.3. Topography and Landscape

The topography of the CEB, shown in Figure 5, declines from all directions towards the lowest point of north-central Namibia, the Etosha Pan, with a minimum elevation of about 1080 m above sea level. Generally, the landscape of the CEB consists of gently undulating broad sandveld of low relief averaging 1110 m above sea level between King Kauluma in the East and Omutsegonime in the northwest.

The Mangetti Duneveld in the north-east is characterized by elongated east-west trending paleo-dunes, extending over a distance of 150 km into the Okavango region. Inter-dune valleys, scattered pans and drainage lines filled with clayey sands are typical of the entire eastern Kalahari but largely limited by the Omuramba Owambo to the thick calcrete cover of the karstveld in the south.

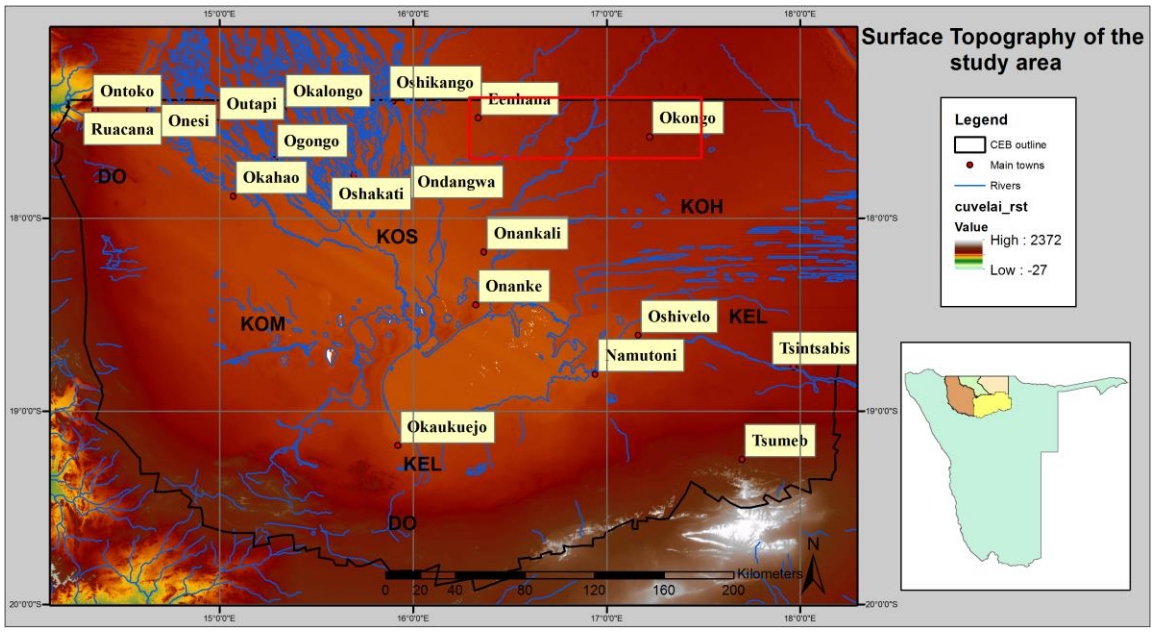

Figure 5. Elevation of the CEB based on data in geodatabase at DWAF.

The southern part of the CEB has an abundance of saline and treeless pans and surrounding plains, which indicates a general flat area (Bittner, 2006). In the western Kalahari, however, remnants of old water courses that receive water periodically during the few rainfall events are also present in this relatively dry area.

3.4. Geology

The CEB is situated in the intra-continental Owambo Basin and was formed during post-cretaceous tectonic development of Southern Africa (Walzer, 2012 after Miller, 2008). This basin is a sub-basin of the wider Owambo Basin. The CEB has been filled with various sediments at very mixed sedimentation rates throughout its geological history. Miller

(1997, 2008 and 2010) mapped and interpreted the geology of the Owambo Basin and his findings will be summarized here.

The geology of the Ovambo Basin contains rocks formed during the formation of the Damara Sequence, the Karoo Sequence and finally the Kalahari Sequence. These are underlain by Precambrian basement rocks.

Accordng to Miller (2008), the formation of the Damara Seequence began with the breakup of Rodinia which was characterized by rifting, spreading and collison (to form Gondwana). During this successive events, First Nosib Group rocks were deposited after which a stable platform was formed on which dolomites and limestones were deposited forming the Otavi Group (730 – 700 Ma ago). The collision and subsequent formation of Gondwana lead to the folding and tilting upwards of the then formed dolomites and limestones along the edge of the Owambo basin, forming a rim to the basin. The rim now forms the mountains around Tsumeb, Otavi and Grootfontein. About 650-600 Ma ago, the mountain belts experienced erosion which was followed by the deposition of the Mulden Group.

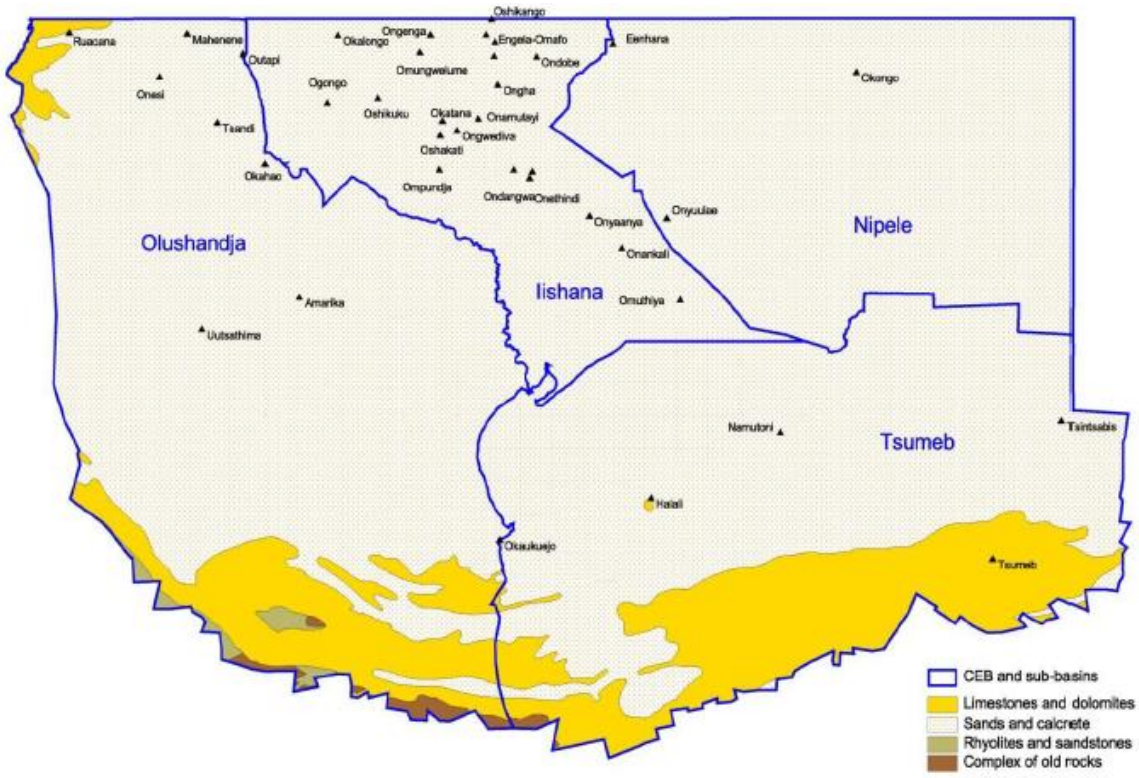

Figure 6. Simplified geological map of the CEB (from Hamutoko, 2013 after Aune, 2011 and Nakwafila, 2011).

During the Dwyka glacial period at about 300 Ma ago, Namibia as well as the Owambo Basin was also affected. The deposition of Karoo sediments started during this time. The Dwyka Formation, caused by the glacial period, is overlain by the Prince Albert Formation which started when glaciers began to melt and retreat due to warmer climates. As the sea level raised, carbonaceous shales, sandstones, siltstones and beds of organic matter derived from plants were deposited in the basin. During early Permian and end of Triassic dessert conditions prevailed which were characterized by the deposition of aeolian sandstone resulting in the formation of the Etjo Formation.

The Owambo basin has been filling up with sand, silt and clay for the past 70 Ma that was eroded from higher grounds surrounding the area. A succession of up to 600 mm thick, semi-consolidated to unconsolidated sediments of the Kalahari Sequence overlay the intrusive and extrusive rocks of Karoo age. The sediments resulted from the erosion of mountains in Central Angola but also from reworked Kalahari sediments. According to Mendelssohn (2000) cycles of climate with wet and dry periods followed each other. Rivers in the area drained into the basin and deposited sediments that formed the Ombalantu, Beiseb, Olukonda and Andoni Formations (Walzer, 2010 after Miller, 2008). These four Formations represent the youngest unit of the basin – the Kalahari sequence with Ombalantu representing the base and Andoni the top. Table 2 shows the stratigraphic column of the Kalahari Sequence.

Table 2. Stratigraphic column of the Kalahari Sequence (from Hamutoko, 2013 after Ploethner et al., 1997 and GWK & Bicon, 2003 and Bittner, 2006)

System	Sequence (AGE)	Formation	Lithology	Maximum thickness (m)
Quartenary	Kalahari Sequence (>120Ma)	Aluvium	Calcrete, Sand	n/a
Tertiary		Etosha Limestone Member	Limestone, Calcrete, Sand	100
		Andoni	Sand, sandstone, Silt	275
		Olukonda	Sand, sandstone, silt	175

System	Sequence (AGE)	Formation	Lithology	Maximum thickness (m)
		Beiseb	Sandstone, mudstone, gravel	50
Cretaceous		Ombalantu	mudstone	100

3.5. Hydrogeology

3.5.1. Regional Aquifer System

All groundwater within the CEB have been established to have a flow directed towards the Etosha Pan, due to its structure. Three groundwater systems have been identified in the CEB:

- Groundwater that is recharged in the fractured dolomites of the Otavi mountain Land at the Southern and Western rims of the basin.
- This groundwater flows northwards, feeding the aquifers of the Karoo and Kalahari sequences. The deep seated multi layered aquifer system which flows from Angola in the southern margin towards Etosha and the Okavango region.
- The shallow Kalahari aquifer in the central part of the CEB which consists of saline water and originates from regular floods.

Bittner (2006) summarized the different aquifers in the CEB into six main groundwater aquifer systems (Figure 7) as follow: the Otavi Dolomite Aquifer (DO) located on the western and southern rim, the Etosha Limestone Aquifer (KEL), the Oshivelo Multi-Layered Aquifer (KOV) in the eastern area, the Ohangwena multi-Layered Aquifer **(KOH)** in the north-eastern parts, the Oshana Multi-layered Aquifer (KOS) covering the area of the Cuvelai drainage system and the Omusati Multi-zoned Aquifer (KOM) situated in the west adjacent to the (KOS). The Ohangwena Multi-Layered Aquifer is of interest in this study and will be described in the next section.

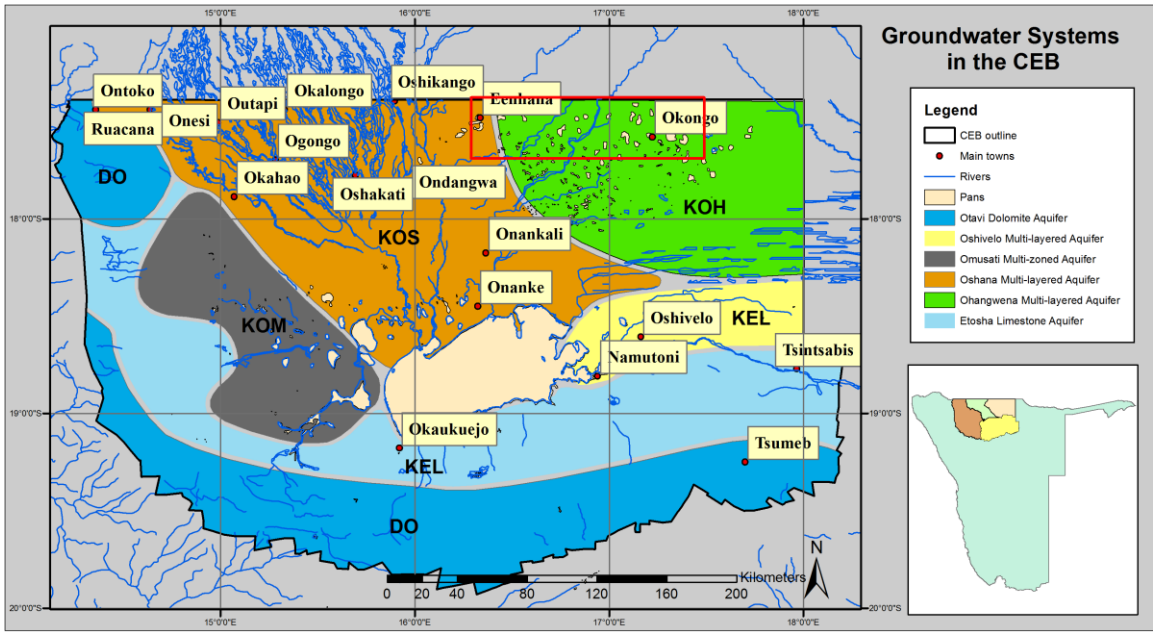

Figure 7. Main groundwater systems of the CEB (modified after Bittner, 2006).

3.5.2. Ohangwena Aquifer System

The Ohangwena Aquifer is a continuous porous aquifer system of the eastern Ohangwena and northern Oshikoto regions. The aquifer is multi layered in that it contains a shallow

perched Ohangwena 0 aquifer (KOH-0) underlain by the Ohangwena I aquifer (KOH-1) and which is in turn underlain in its western, brackish to saline part by the Ohangwena II aquifer (KOH-2). Figure 8 outlines a simplified cross sectional view through the Ohangwena Multi-Layered Aquifer.

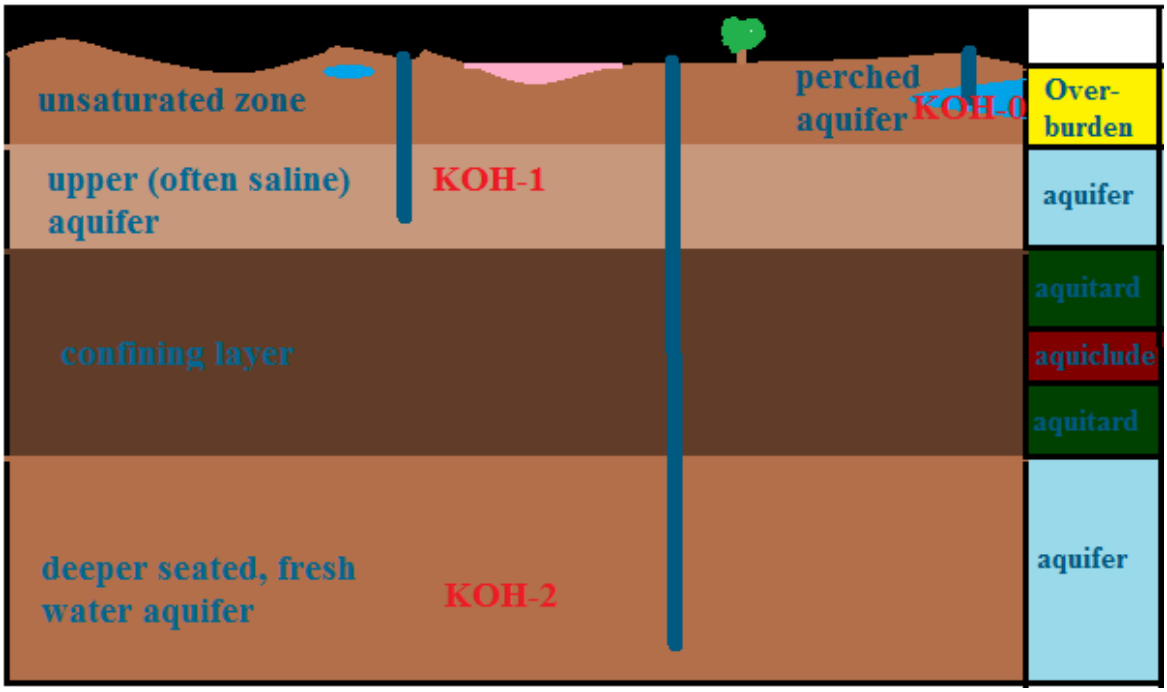

Figure 8. Cross sectional view through the Ohangwena Multi-Layered Aquifer showing positions of KOH-0, KOH-1 and KOH-2 in the subsurface (modified after BGR, 2009).

KOH-0 is the aquifer of interest in this study. This aquifer is not a single aquifer, but is a series of small perched aquifers occurring predominantly in the Kalahari covered area north-east of Okankolo (Christelis et al., 2011). The aquifers are mainly recharged by direct infiltration of rainwater and are exploited by means of ‘omufima’ (funnel-shaped dug well)

in shallow areas and ‘ondungu’ (cylindrical-shaped hand-dug well) in areas where these aquifers are at depth (see Figure 9).

Figure 9. Types of hand dug wells (left: ondungu; right: omufima) (from Hamutoko, 2013).

4. Methodology

4.1. Review of Existing Borehole Logs

A total of 46 existing borehole lithology logs were carefully reviewed to locate aquifer and aquitard layers. These boreholes were previously drilled for the Department of Water Affairs and Forestry (DWAF) in co-operation with the Federal Institute of Geosciences and Natural Resources of Germany (BGR) for groundwater monitoring as well as for rural water supply. In order to locate the possible water bearing layers and aquitard layers, the logs were compared to existing geological information available in the area as well as literature describing the textural features geological materials.

The geological information derived from the logs and used to identify the perched aquifer and the aquitard below it, were:

- type of lithology,
- grain size,
- degree of sorting, and
- type of matrix

The thickness of the layers were also noted. Figure 10 shows an example of the lithology logs that were used.

Borehole log, WW 200470, Ohangwena Region

WW No	No	Farm				LAT_DD	LON_DD	Drill depth	Collar elevation from SRTM
						Schwarzeck		[m]	[m]
200470	MLRS 3	1987				-17.64003	17.74989	150	1156.7

Section	Thickness	Elevation	Litholog			
[m]	[m]	[m]	Rock	Colour	Grain size	Description
0-3	3	1157-1155	Sand	lt rd-yel	silt-fgr	Moderate sorting, mainly fgr, minor silt and mgr fractions, grains subangular to well rnded, aeolian?
-18	15	-1140	Sand	lt yel	silt-fgr	Moderate sorting, mainly fgr, minor silt and mgr fractions, grains subangular to well rnded
-32	14	-1126	Sand	rd	silt-fgr	Moderate sorting, mainly fgr, minor but variable silt and mgr fractions, rare cgr grains, grains subangular to well rnded, becomes gradually lt yel or lt reddish-yel downwards
-60	28	-1098	Sand	v lt yel	silt-fgr	Variable sorting, v minor but variable mgr fraction, rare cgr grains, grains subangular to well rnded, v calcareous with small wht calcrete nodules from 1118-1098 m, small hard buff calcareous dolocrete nodules at 1102, 1100 m, larger nodules 1099-1098 m
-84	24	-1074	Sand	off wht	silt-fgr	Variable sorting, v minor but variable mgr fraction, rare cgr grains, grains subangular to well rnded, highly calcareous, sl less calcareous from 1088-1077 m, small hard buff calcareous dolocrete nodules at 1097 m, small hard buff silcrete nodules at 1075-1074 m, v v lt gm calcareous silt layer at 1077 m
-86	2	-1072	Sand	v lt gm	fgr	Sl clayey v calcareous fgr sand
-102	16	-1056	Sand	off wht	silt-fgr	Variable sorting, v minor but variable mgr fraction, rare cgr grains, grains subangular to well rnded, highly calcareous, small hard buff calcareous dolocrete nodules at 1060-1059 m, pink v calcareous clayey silt layer at 1058 m
-150	48	-1008	Clayey sand	pink	clay-fgr	Variable sorting, v minor but variable mgr fraction, grains subangular to well rnded, silt fraction variable, clay content variable, v clayey at 1055, 1052-1050, 1048, 1037-1036, 1030-1028 m, lt rd at 1047-1045 m, highly calcareous, small soft white calcrete nodules scattered throughout, a hard buff calcareous dolocrete nodule at 1055 m, in places small patches of wht sand cemented by calcareous dolocrete, interbedded layers of off wht, highly calcareous f- to mgr sand with rare cgr grains from 1017-1008 m

Sand almost pure quartz sand, many larger grains very well rounded — Logged by R. Miller

Figure 10. Borehole lithology log for WW200470, used to identify the different hydrogeological layers of interest (source DWAF).

Using standard hydraulic conductivity tables (available in Appendix C), estimated values of hydraulic conductivity were given for the perched aquifer and aquitard based on texture, degree of sorting and silt content.

4.2. Soil Sampling

Soil samples were collected at depth, close to borehole WW201633 as well as in an ephemeral river bed between Okongo and Eenhana by Matthias Beyer and Marcel Gaj. These samples were collected with the use of a hand auger. The soil sample from the vicinity of borehole WW201633 were taken at an interval of 10 cm from 10 cm up to the

depth of 7.4 m. Between 5.1 and 5.5 m and between 6.6 and 6.9 m a cobra drill was used to drill through the subsurface. No samples were collected between 5.7 and 6.5 m.

In the ephemeral river bed, soil samples were taken at random depths up to 2 m below the surface. Here, only a hand auger was used. In addition to these samples, a set of samples collected by BGR during the drilling of the monitoring boreholes at Oshandi for the deeper aquifers were also received from them for analysis. The received samples were those taken from borehole WW 202670 at depths from 1 – 30 m. The collected soil samples were used to define these specific depth zones of KOH-0 in terms of texture and hydraulic conductivity.

4.3. Grain Size Analysis

A portion of the soil samples collected from the vicinity of borehole WW201633 at 10 – 150 cm depth were analyzed at the University of Namibia's Petrography Laboratory using the sieving method. In the Petrography Laboratory, the samples were first weight and dried in the oven over 24 hours at a temperature of 105^{o}C and then weight again after drying using a weighing balance (Figure 11).

After the samples were dried, they were passed through a set of sieves with mesh sizes in the order from 2 mm, 1 mm, 500 µm, 250 µm, 150 µm and 63 µm (see Figure 12). This process was done to separate the soil samples into different fractions according to the sieves used. After this, the mass of soil particles retained on each sieve was obtained using the weighing balance and cumulative percentages of the grain sizes were calculated. The cumulative percentages of the different grain sizes (i.e. 2 mm, 1 mm, 500 µm, 250 µm, 150

µm and 63 µm) were then used to plot grain size distribution curves which were used to calculate the hydraulic conductivity for each soil sample collected.

Figure 11. Soil samples in trays (A), soil samples in the oven (B) and soil sample being weight (C).

Figure 12. Electric shaker with standard set of sieves.

According to Freeze and Cherry (1979), hydraulic conductivity is related to grain size distribution of porous media. This interrelationship is a very useful tool in the estimation of hydraulic conductivity of aquifers in areas where direct permeability data is sparse or non-existent.

The Beyer (1964) equation was used to estimate the hydraulic conductivities of the soil samples based on the resultant grain size distribution curves. The Beyer equation is given by:

$K = C_{Beyer} * d^{10}$ where $C = 0.012 * U^{-0.2052}$

and U is the uniformity coefficient given by $U = \frac{d_{60}}{d_{10}}$ where d_{60} and d_{10} represent the grain diameter in mm for which 60% and 10% of the sample are finer than obtained from the grain size distribution curves for each sample. The resultant grain size distribution curves for the analyzed samples can be found in Appendix A.

The remaining soil samples collected close to borehole WW201633 from 10 – 740 cm as well as those collected in the ephemeral river between Okongo and Eenhana were analyzed in Germany using the Camsizer method. The CAMSIZER (see Figure 13) is a compact laboratory instrument used for the simultaneous measurement of particle size distribution, particle shape and additional parameters of powders and granules.

Figure 13. The particle analyzer CAMSIZER XT, for wet and dry measurements (Retchs Technology, 2015).

In the CAMSIZER, the sample is transported to the measurement field via a vibratory feeder where the particles drop between planar light sources and two cameras. The projected particle shadows are then recorded at a rate of more than 60 images per second and analyzed. This allows for the recording and evaluation of every single particle in the bulk material flow and it is therefore possible to measure a wide range of particles from 20 µm – 30 mm.

After particle size analysis of these samples, the resultant results were used to calculate the hydraulic conductivity values of the soil samples using Hazen, Seelheim, Bialas and Beyer. All these were done in Germany at the BGR Laboratories.

The Hazen equation used, also described in chapter 2, is given by:

$$Kf = C * d10^2$$

where C is an empirical constant and d10 represents the grain diameter for which 10% of the sample are finer than.

The Seelheim equation used to calculate hydraulic conductivity is given by:

$$Kf = 0.00352 * d50^2$$

where d50 represents the grain diameter for which 50% of the sample is finer than.

The Bialas equation used is given by:

$$Kf = 0.0036 * d20^{2.3}$$

where d20 represents the grain diameter for which 20% of the sample is finer than.

The Beyer equation was also further used to calculate the hydraulic conductivity values using the particle size distribution results obtained.

The set of samples, collected during mud rotary drilling of monitoring boreholes at Oshandi by BGR, were analyzed for grain size distribution using the sedimentation method. For this method, a 500 ml cylinder (shown in Figure 14) was filled with tap water and 20 g of sample material was added. The sample was shaken for several seconds and the material was allowed to settle. The temperature of the tap water used determined the time at which samples were to be taken from the sedimentation cylinder.

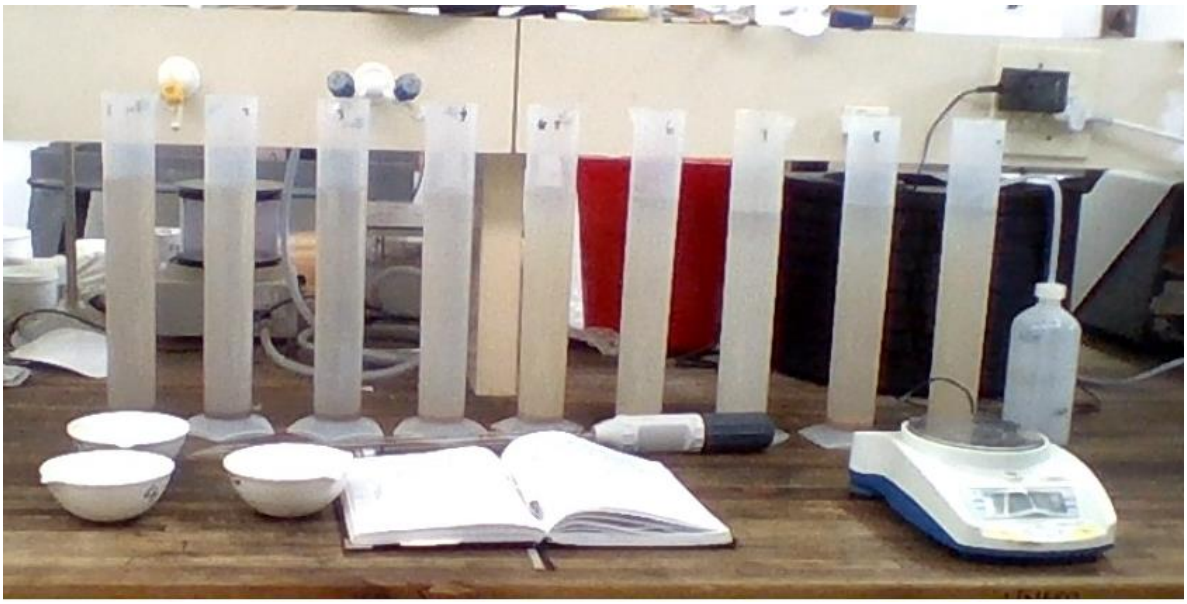

Figure 14. Materials used in the sedimentation method (500 ml cylinder, pipette, weighing balance and evaporating dishes).

At 50 seconds, the first sample which represents the amount of silt and clay in the 20 g soil sample was taken using a pipette. The second sample, which determines the amount of clay, was taken on average after 6 hours and 30 minutes. The samples taken from the sedimentation cylinder were placed in the oven over 24 hours to evaporate and weighed to determine the amount of silt and clay at each depth.

The Soil Water Characteristic Program (SPAW) was used to estimate hydraulic conductivities of the samples analyzed using the sedimentation method. This program uses the percentages of clay and sand portions of the sample to determine its soil type and soil water characteristics as well as the hydraulic conductivity (see Figure 15).

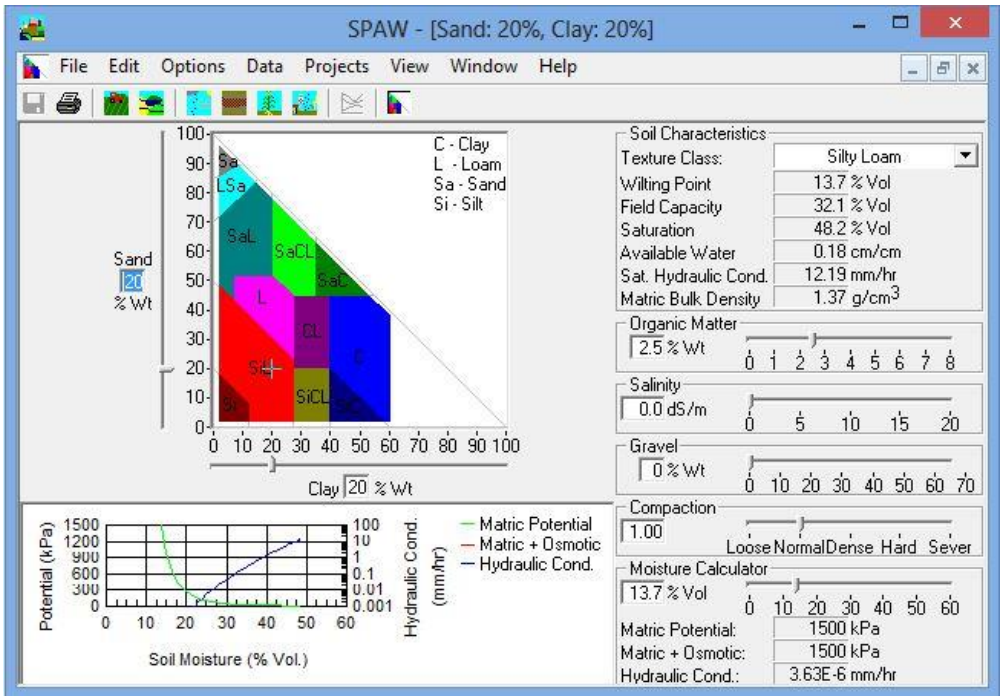

Figure 15. SPAW program window (Saxton, 2013).

4.4. Porosity and Coefficient of Uniformity

The porosity of KOH-0 material was determined from Laboratory analysis carried out by Hamutoko (2013). The equation used to compute for porosity is given by:

$$n = \frac{100V_V}{V}$$

where n is the porosity in percentage, V_v is the volume of void space in a unit volume of the material and V is the unit volume of the material including the voids and solids.

The uniformity coefficient (U) of a sediment is a measure of how well sorted or poorly sorted it is (Fetter, 2001). This coefficient is calculated by dividing the weight of the grain size that is 60% finer (d60) by the weight of grain size that is 10% finer (d10). That is:

$$U = \frac{d60}{d10}$$

Samples with U less than 4 are classified as well sorted whilst those with U more than 6 are classified as poorly sorted.

4.5. Estimation of Possible Vertical and Horizontal Groundwater Flow

To evaluate the amount of flow from KOH-0 into KOH-1 it was important to establish the direction and magnitude of the vertical hydraulic gradient across the aquitard that separates these units. The presence of a strong downward gradient indicates a potential presence of a deep pathway for groundwater flow from KOH-0 to KOH-1. In principle, in order to get more accurate estimates for the amount of flow through the aquitard, the vertical gradient should be assessed by simultaneous measurements of hydraulic heads in the KOH-1 wells and nearby wells completed in KOH-0.

Figure 16 is a simple representation of the groundwater flow components in the KOH aquifer system between KOH-0 and KOH-1. Five boreholes screened through KOH-1 and five hand dug wells dug through KOH-0 were used to estimate the vertical hydraulic gradient across the aquitard. A simplified cross sectional area of 1 m^2 was assumed for the area over which groundwater from KOH-0 may enter the aquitard via leakage. The aquitard hydraulic gradient used in this calculation was estimated from comparison of the reported textures and degree of sorting of the aquitard material against standard hydraulic conductivity tables of known geological materials.

The resultant Darcy equation used in the evaluation for vertical flow through the aquitard is:

$$Q_{aquitard} = K_{aquitard} I_{aquitard} A_{aquitard},$$

where Q indicates groundwater flux through the aquitard, K is the hydraulic conductivity of the aquitard, I is the hydraulic gradient across the aquitard and A is the cross sectional area assumed for flow.

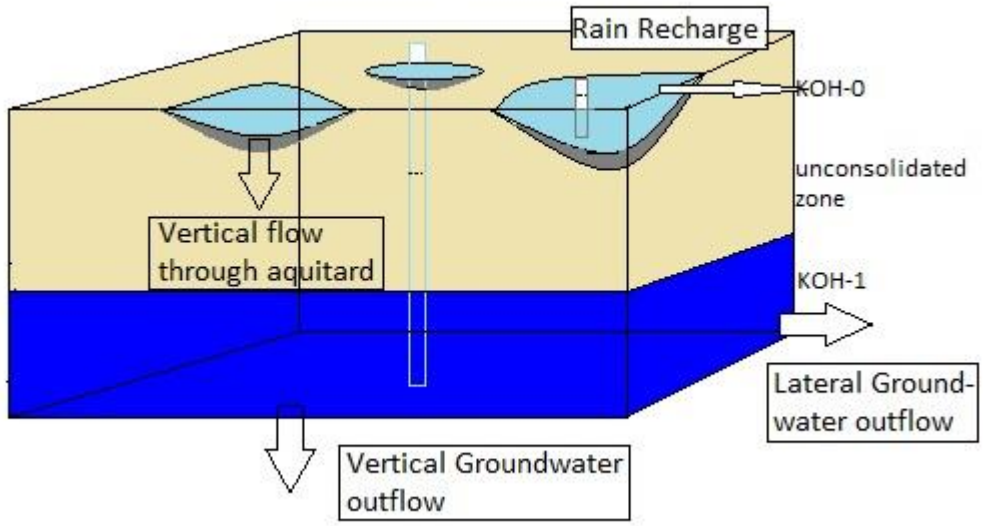

Figure 16. Groundwater Components (KOH-0 and KOH-1).

To evaluate the significance of the vertical flux through the aquitard, it was important to also compute the horizontal flux through KOH-1. The same equation for Darcy's law was used for the horizontal flux through KOH-1. The hydraulic conductivity of KOH-1 was computed from transmissivity values determined by van Wyk (2009) using the following equation:

$$T = Kb,$$

where T represents the transmissivity of the aquifer, K is the hydraulic conductivity of the aquifer and b is the thickness of the aquifer. The hydraulic gradients in KOH-1 were estimated from water table elevation contour maps of the aquifer. From Literature, it is known that groundwater within the KOH system has a lateral flow from Angola in a southerly direction towards the Etosha Pan (see Figure 17). The northern boundary of the Niipele Sub-basin was thus assumed to be the inflow boundary for KOH-1. The estimated cross sectional area available for groundwater flow was therefore calculated by multiplying the entire northern boundary of the Niipele Sub-basin with the thickness of KOH-1. Figure 18 illustrates the assumed cross sectional area of KOH-1 available for horizontal flow. To obtain the hydraulic gradients within the aquifer, a groundwater elevation contour map was created his using existing borehole data.

Figure 17. Groundwater flow direction in the CEB (modified after Mendelsohn et al., 2013).

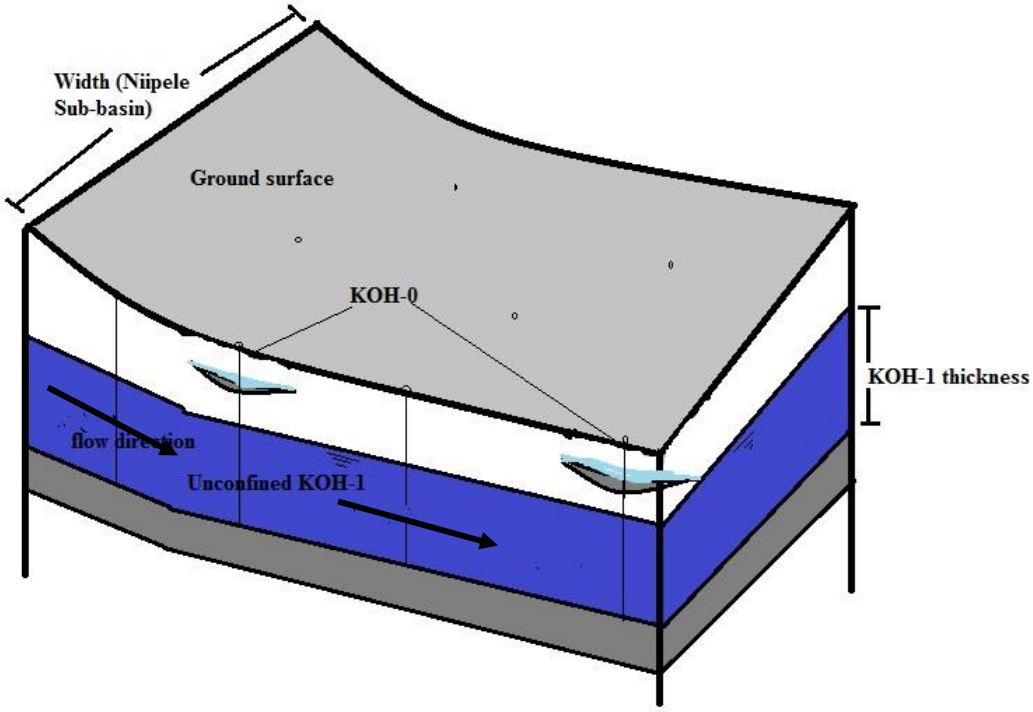

Figure 18. Cross section showing KOH-1 area components.

5. Results

5.1. Field Observations

During field excursions undertaken throughout the study period, observations were made with regards to the set ups of the two types of hand dug wells found in the area. Shallow, funnel shaped hand-dug wells were encountered mostly in depressions and rivers and require re-digging as the water levels decrease or as they fill up with sand over time. The deep, cylindrical shaped wells were found to occur mostly in the sand field, dunes and pans. These do not require re-digging as most are dug up to 30 m depths.

5.2. Overview of Borehole Lithology Logs

Table 5 in Appendix A shows the different textures for KOH-0 and the underlying aquitard which were identified from the lithology logs (example in figure 19). The results presented in the table were combined with the five hydrotopes identified and described by Hamutoko (2013) and Davids (2013) together with other features to produce an aquifer-aquitard-hydrotope map (see figure 20). The boreholes used to create the map are more than 3 km apart, except for the boreholes in Eenhana (WW 201631 and WW 201632) which are approximately 35 m apart and the boreholes in Elundu (WW 203747 and WW 203749) which are 60 m apart.

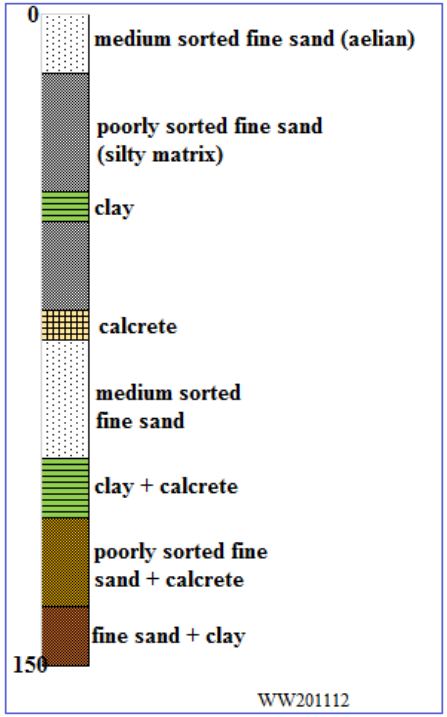

Figure 19. Simplified lithology log for borehole WW201112 with perched aquifer layer being the first medium sorted, fine sand layer from the ground surface and the semi-confined aquifer being the medium sorted fine sand layer below the calcrete (in this litholog).

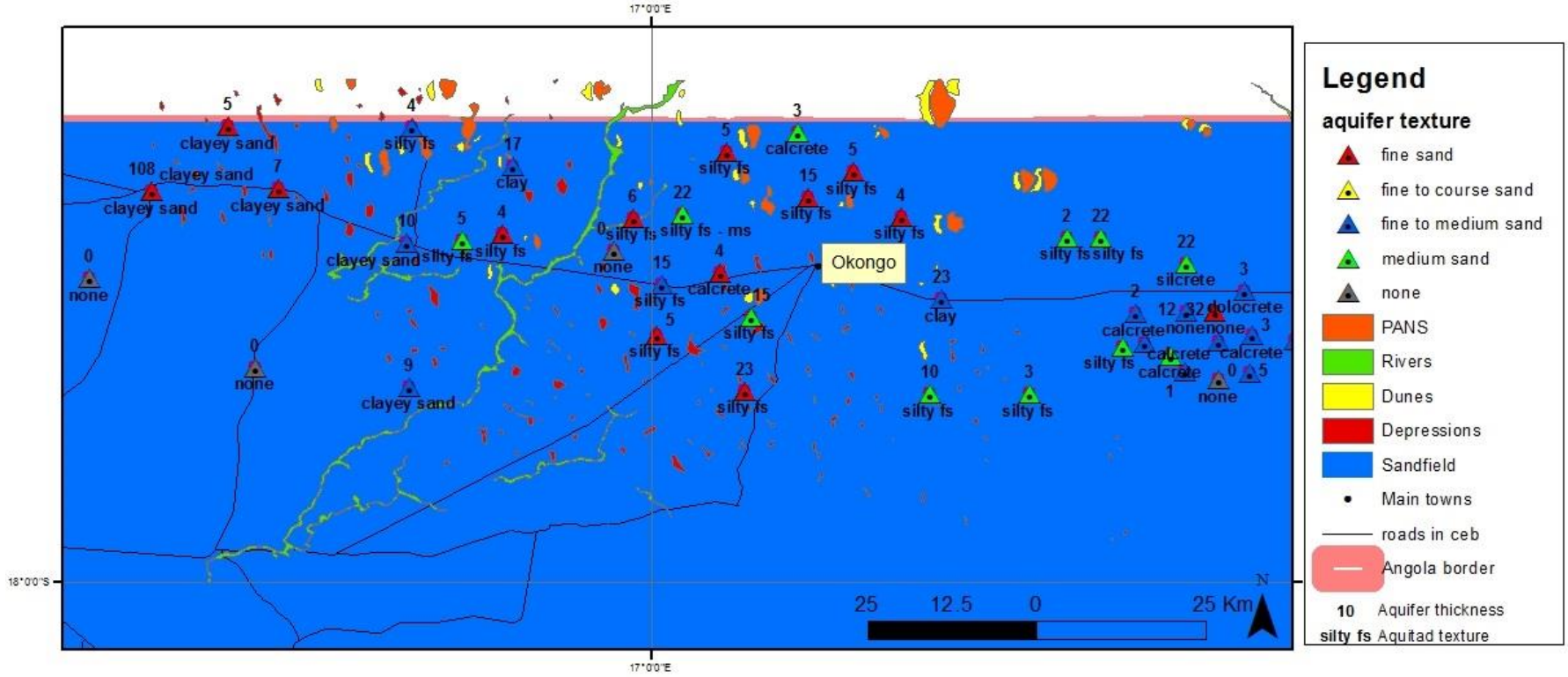

Figure 20. Map showing hydrotopes (from Hamutoko, 2013), aquifer texture and thickness, and aquitard thickness.

The map shows that the entire study area is made up of sand field with the pans, dunes, depressions and rivers occurring as lenses within the sand field. Pans and dunes are seen to occur predominantly in the northern portion of the study area, alongside each other, towards the Angolan border. The depression lenses are found to occur nearly throughout the study area and the rivers make up the known old river channels.

The perched aquifer material is seen in the lithological logs to be the layer from the surface of the ground to some meters below. The perched aquifer is made up of fine to medium sand in the exclusive sand field area whilst in the depression area, the aquifer is mostly fine sand at most sites with fine to medium and medium sand at a minority of the sites. In the river, dune and pan areas, a combination of fine, fine to medium and medium sand can be found.

In the sand field area, the perched aquifer thickness varies greatly between 2 m to more than 30 m. At sites where depressions, pans and dunes are found, the thickness of the perched aquifer range from 2 m to 10 m, only few sites in these areas are found to have thicknesses of more than 10 m. No borehole is found exactly in the river and the surrounding area is mostly sand field with lenses of depressions, pans and dunes. The thicknesses of the perched aquifer determined from the lithologs cannot be used to delineate the lateral extends of the perched aquifer lenses due to the distance between the wells and the great difference in the thicknesses observed in the lithologs. For instance, WW200649 and WW201104 are approximately 8 km apart, however, the thickness of the perched aquifer observed at WW200649 is 15 m and that observed at WW201104 is 4 m,

the aquifer texture at WW200649 is fine to medium sand whilst at WW201104 it is abundantly fine sand.

5.3. Hydraulic Parameter Estimates

5.3.1. Perched Aquifer (KOH-0)

Appendix B contains plots of the grain size distribution curves. Also included in Appendix B are tables of grain size analysis results of the soil samples collected from the three sites described under methodology. The plots of the results from the Eenhana Forest site and those from the Ephemeral river show that a major part of the geological materials fall within the sand size range with grain sizes ranging from 0.1 to 2 mm diameter, which generally coincides with a range of fine to course sand. The samples from Oshandi contain a high percentage of sand with minor silt and clay. A majority of the samples are classified as being loamy sand.

The hydraulic conductivity values of the perched KOH-0 aquifer evaluated from grain size distributions and calculated using four different methods are also summarized in Appendix A under table 11. As mentioned under methodology, Hazen, Seelheim and Bialas were used for the samples from the forest site in Eenhana and those from the Ephemeral River bed. The Beyer formula was used on the samples analyzed using the sieving method in UNAM and also further on the results obtained from Matthias Beyer. The SPAW program was only used on the cohesive samples from the deep borehole in Oshandi.

The hydraulic conductivity values obtained from these methods span between 10^{-6} and 10^{-4} m/sec, with lowest values obtained from the Beyer equation for the samples analyzed using the sieving method at UNAM. Statistical analysis of the hydraulic conductivity values obtained using the five methods resulted in p-values less than 0.05 (see table 3) which means that the standard deviations of these sets of data are not equal and the values obtained are statistically different.

Table 3. Statistical analysis results for Ephemeral river hydraulic conductivity data

Source of Variation	*SS*	*df*	*MS*	*F*	*P-value*	*F crit*
Between Groups	9.63E-07	3	3.21E-07	22.06	6.23E-08	2.90
Within Groups	4.66-07	32	1.45E-08			
Total	1.42E-06	35				

The cohesive samples from the deep borehole in Oshandi evaluated with the SPAW program have hydraulic conductivity values between 1.77E-04 and 3.49E-04 m/sec.

Figure 21, 22 and 23 show scatter plots of hydraulic conductivity (obtained from the different methods) with depth for the perched aquifer materials collected from the three sites. The plot for Eenhana Forest site shows a general decrease in hydraulic conductivity with depth in the first 3 m and a higher conductive layer is encountered at depth of 6.7 m. This is especially clearly visible in the Hazen and Seelheim plots. The hydraulic conductivity is also seen to decrease with depth in the Ephemeral data with a more conductive layer encountered at 1.4 m (shown in Figure 22). A decrease in hydraulic conductivity is observed in the first 4 m of the Oshandi profile (see Figure 23). Here,

hydraulic conductivities are scattered with depth and layers with higher hydraulic conductivities are encountered at depth of 4 m, 17 – 20 m and at 26 m.

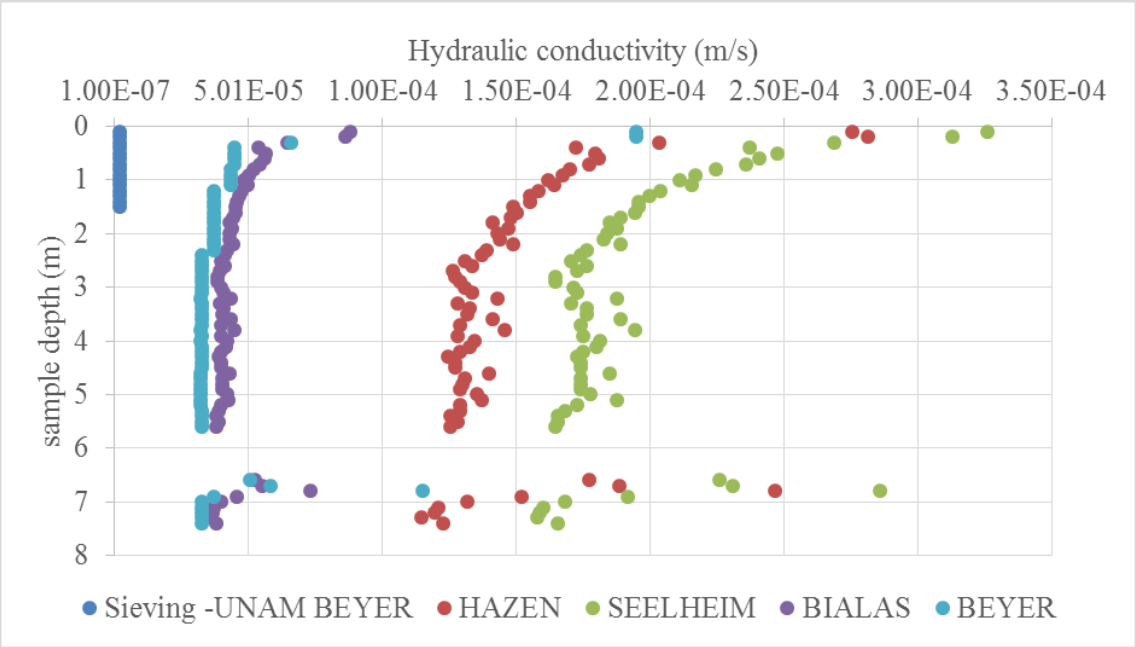

Figure 21. Plot of hydraulic conductivity (estimated with five different methods) versus depth at Eenhana Forest site.

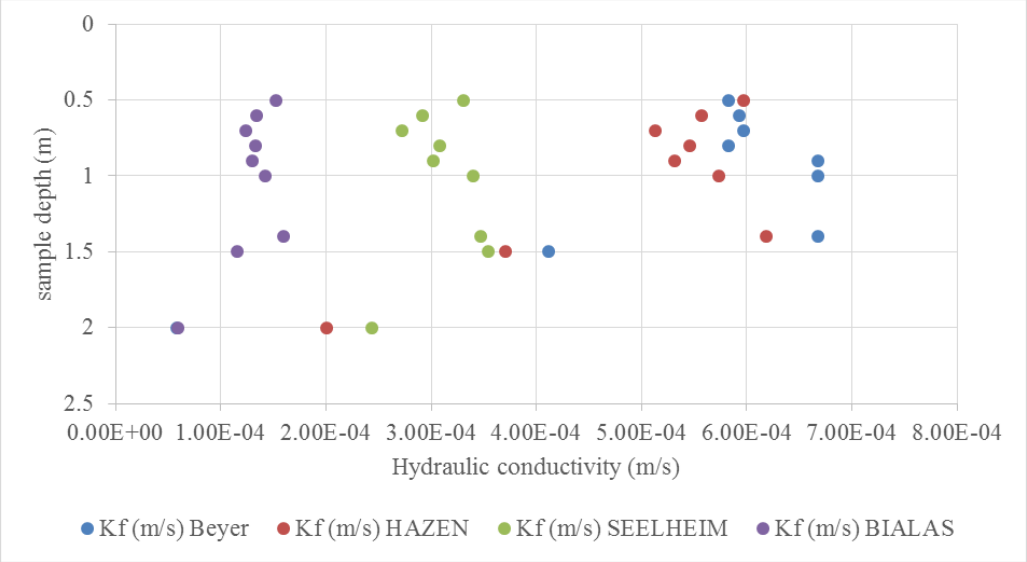

Figure 22. Plot of hydraulic conductivity (estimated with four different methods) versus depth at the Ephemeral River site.

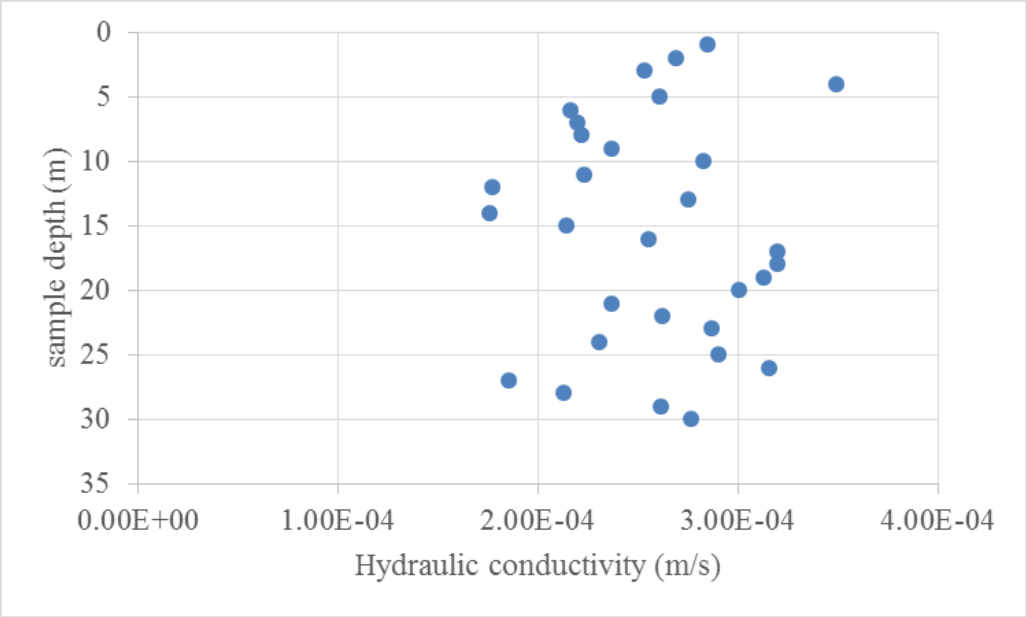

Figure 23. Plot of hydraulic conductivity (estimated using the SPAW) versus depth of the samples from the deep borehole at Oshandi.

The minimum hydraulic conductivity values for KOH-0 estimated from existing borehole lithology logs are given in table 6 in Appendix A. The relative hydraulic conductivity values based on texture and degree of sorting of the KOH-0 aquifer material ranges between 1.2E-4 m/sec and 2.9E-4 m/sec. Lower hydraulic conductivity values are estimated for areas where the aquifer material consist of silt.

Figure 24 is a representation of the spatial distribution of hydraulic conductivity (estimated using documented standard hydraulic conductivity tables) of the perched aquifer at each borehole as given in Table 6 (Appendix A). Relatively high hydraulic conductivity values of the perched KOH-0 are encountered in the boreholes around Okongo. The values are randomly distributed, however they are of the same magnitude with very little difference between them.

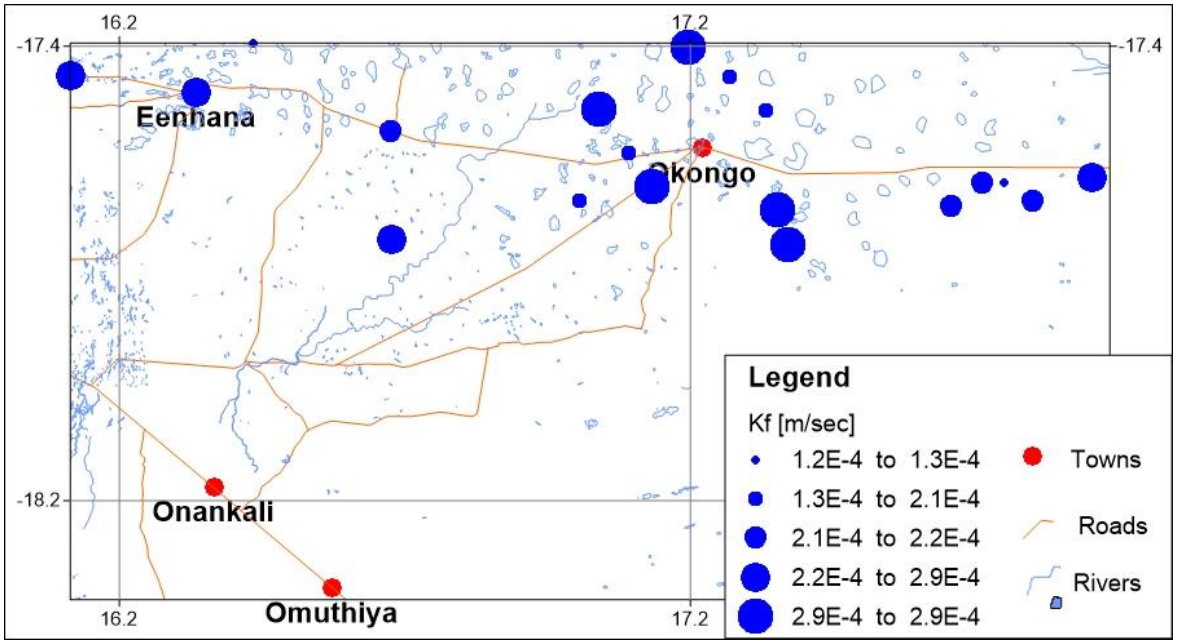

Figure 24. Map showing the spatial distribution of minimum hydraulic conductivities of KOH-0 based on texture and grain sorting.

Table 4. Effective porosity and Coefficient of uniformity of KOH-0 material with depth based on analysis of raw data from Hamutoko (2013)

Site	depth (cm)	Effective porosity (%)	Uniformity coefficient
Epembe sand field	25	6.1	2.3
	65	8.3	2.8
	140	9.5	3.6
	200	11	3
	275	16	25
Between Omboloka and Eendobe	20	1.4	3.5
	70	1.6	0.3
	130	2.3	0.3
	205	2.4	0.3
Oshana-shiwa	0	1.4	3.0
	40	5.3	3.6
	80	6.2	3.7
Omboloka dunes	0	0.4	2.0
	60	2.6	2.4

Table 4 contains the results of porosity and the uniformity coefficient for KOH-0 determined from raw data sourced from Hamutoko (2013). Four Sample sites are presented, namely, Epembe sand field, site between Omboloka and Eendobe, Oshana-shiwa and Omboloka dune. The deepest depth at which samples were collected is 275 cm.

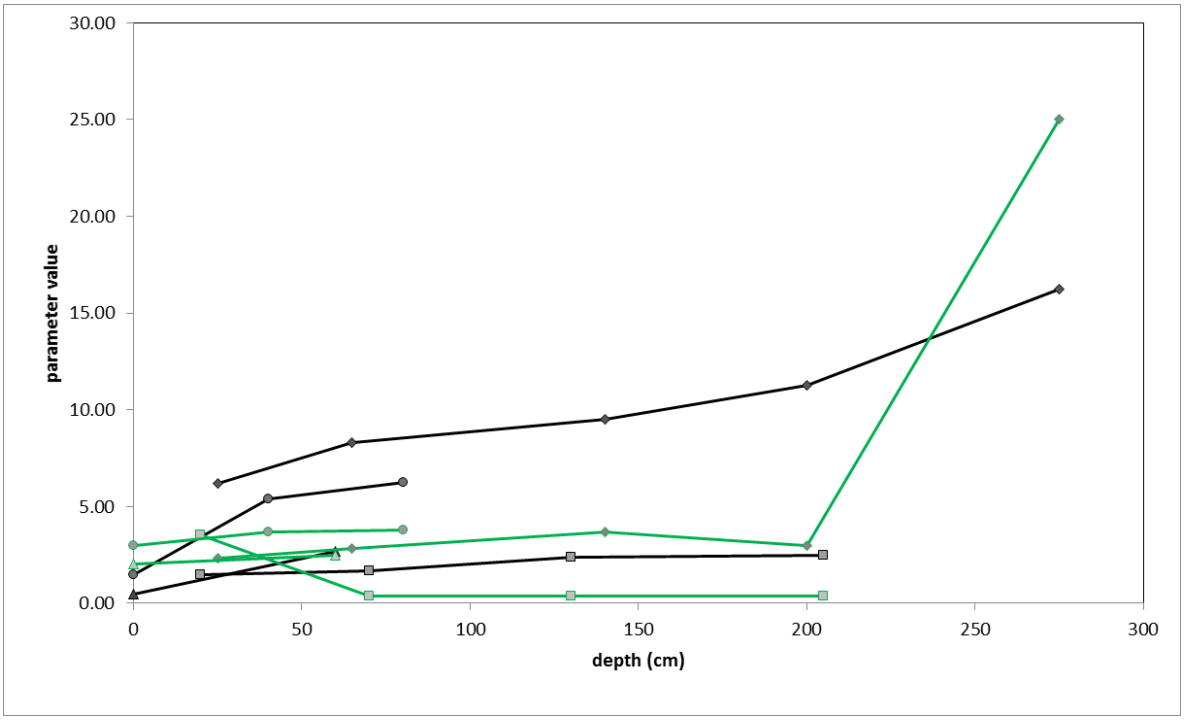

Figure 25. Graph of effective porosity and uniformity coefficient of materials with depth. Uniformity coefficient is presented in green, whilst effective porosity is in black; shapes: diamond represents Epembe sand field site, square represents the site between Omboloka and Eendobe, circle represents Oshana-shiwa and triangle represents Omboloka.

The graphs of porosity and uniformity coefficient with depth for each site are shown in Figure 25. From the graphs it can be seen that as the depth increases, the porosity increases. The graphs for the coefficient of uniformity observed for these profiles show that the materials fall within the well sorted range except for one sample collected at Epembe sand field at 275 cm whose uniformity coefficient equals to 25.

5.3.2. Aquitard

Table 7 in Appendix A. shows the minimum hydraulic conductivity values for aquitard layers based on the texture and degree of sorting, as identified from the borehole lithology

logs. The aquitard is multi-layered in nature and contains alternating layers of silty sand, clayey sand, clay and calcrete. The minimum hydraulic conductivity in this multi-layered aquitard is estimated to be in the range of 3.17E-09 m/sec and 1.90E-04 m/sec. The lowest values in this case are those of the impermeable to very low permeable layers such as calcrete and the highest are the poorly sorted fine to medium grained sand layers.

Using the results given in table 7, a minimum aquitard hydraulic conductivity spatial distribution map was created for the study area (see Figure 26). From the map it can be seen that the hydraulic conductivity of the aquitard in the area where most hand dug wells are found, is mostly in the range of 1.3E-04 m/sec to 1.9E-0.4 m/sec. In this area the aquitard is made up of thick poorly sorted fine grained sand with minor silt.

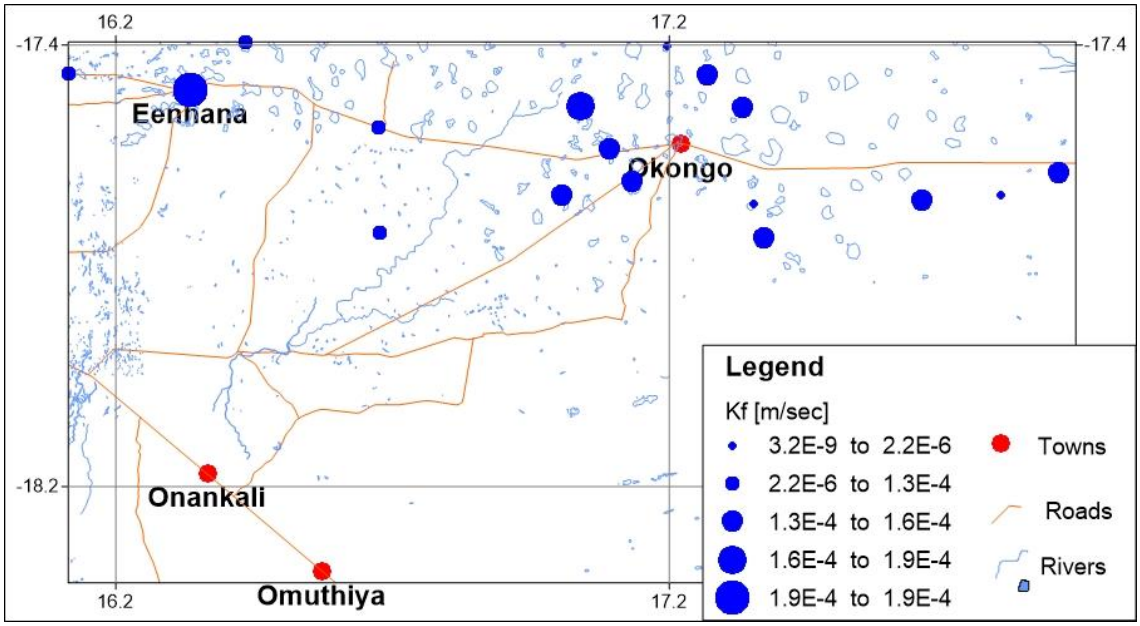

Figure 26. Spatial distribution map of minimum hydraulic conductivity for the aquitard based on textures and grain sorting.

5.4. Groundwater Seepage and Flow

Table 12 in Appendix D summarizes sites which were used to estimate the seepage from KOH-0 to KOH-1 through the aquitard. Also shown in the table are the values for hydraulic conductivity and hydraulic head at each site as well as the assumed cross sectional area of flow. Ideally, the vertical gradient across the aquitard needs to be assessed by simultaneous measurements of hydraulic heads in wells not more than a few meters apart from each other. However, due to a limited number of well points, the hand dug wells and boreholes used here are more than 3 km apart. From the table it can be seen that the hydraulic head in KOH-0 is higher than the head in KOH-1 (also illustrated in Figure 27). The head difference therefore indicates a downward directed vertical component of the groundwater flux through the aquitard from KOH-0 to KOH-1.

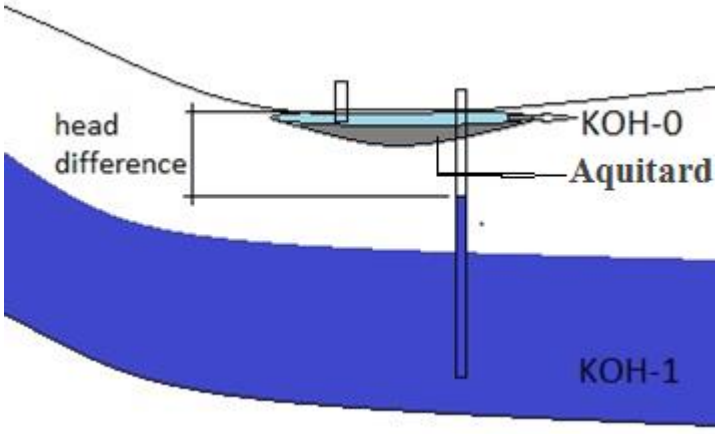

Figure 27. Head difference between KOH-0 and KOH-1 across the aquitard.

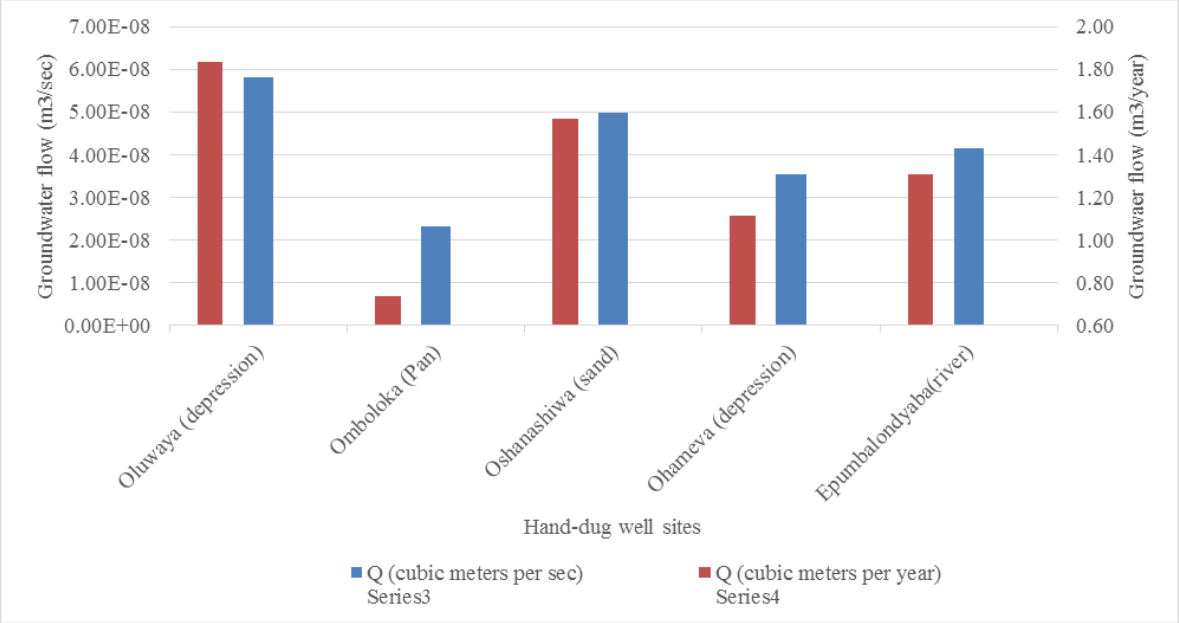

Figure 28. Column chart for possible amount of groundwater flow through the aquitard.

The amount of groundwater flow from the perched KOH-0 to KOH-1 estimated using Darcy's law ranges between 2.33E-08 to 5.82E-08 m^3/sec for every square meter (as seen in in Figure 28). Assuming that groundwater seeps through the aquitard layer all year round, the amount of seepage would range from 0.735 m^3/year to 1.83 m^3/year for every square meter.

Figure 30 shows the equipotential map created from hydraulic head data from selected KOH-1 boreholes in the study area. A groundwater mount is indicated in the area north of Okongo has a south-eastern flow from central northern part of the study area. Also, the water table contours are much more closely spaced in the area north of Okongo, which indicate higher hydraulic gradients in this area. For this reason, a maximum and minimum estimated value for the hydraulic gradient was determined for the study area as well as an

actual hydraulic gradient at each borehole. The estimated hydraulic gradients are given in Table 14 in Appendix D. Also shown in the table is the hydraulic conductivity, aquifer thickness and the estimated cross sectional area of flow. The hydraulic conductivity was determined from transmissivity values of KOH-1 published by van Wyk (2009).

In the study area a maximum groundwater gradient of 0.00193 m/m is estimated for KOH-1 and a minimum of 0.000193 m/m. The inflow boundary (northern boundary of Niipele Sub-basin) was measured with the measuring tool in ArcMap 10.1 (Esri, 2012) and was found to be approximately 188 564 m wide. On average, KOH-1 is about 40 m thick with an average hydraulic conductivity of 6.02E-06 m/sec. The amount of flow within KOH-1 is therefore estimated at 6700 m^3/day, in areas of high hydraulic gradient and 690 m^3/day in areas where the hydraulic gradient is relatively lower.

The estimated amount of flow through KOH-1 at the given sites is presented in Figure 29. For this cross sectional area, the estimated maximum lateral flow through KOH-1 is 4370 m^3/day and the minimum amount of flow is 371 m^3/day. If this condition occurs all year (365 days), the amount of flow would range between 1.35E+05 and 1.59E+06 m^3/year.

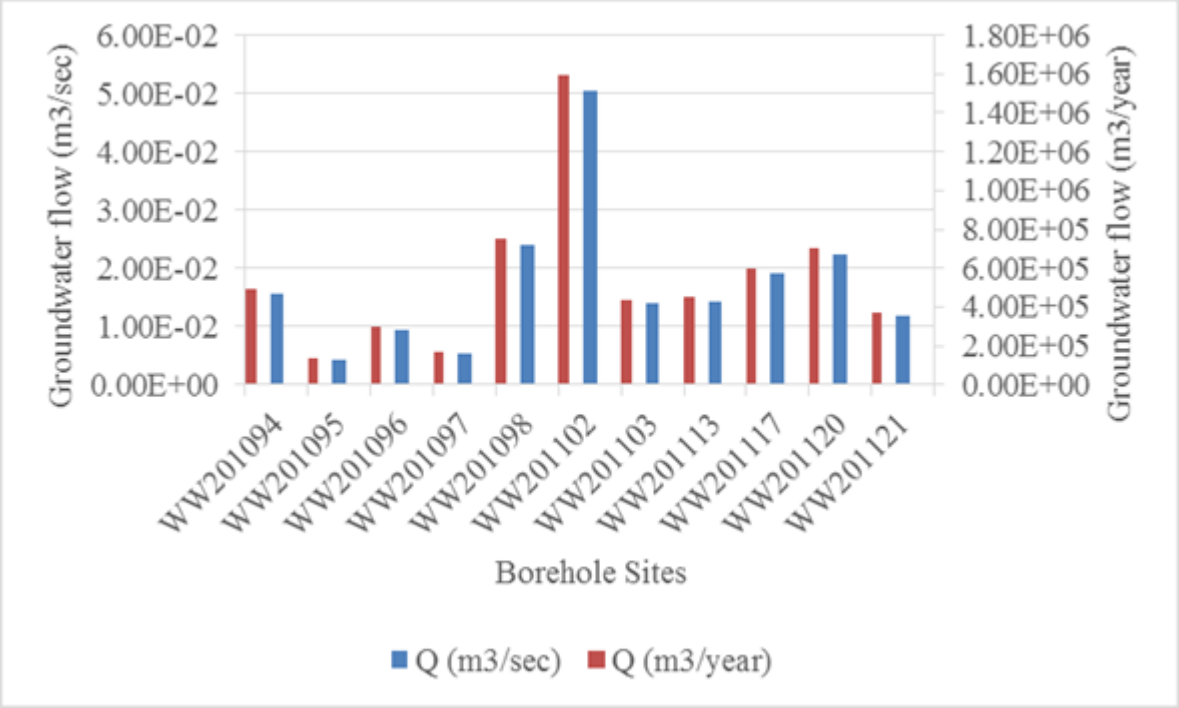

Figure 29. Estimated groundwater flow within KOH-1 at selected borehole sites.

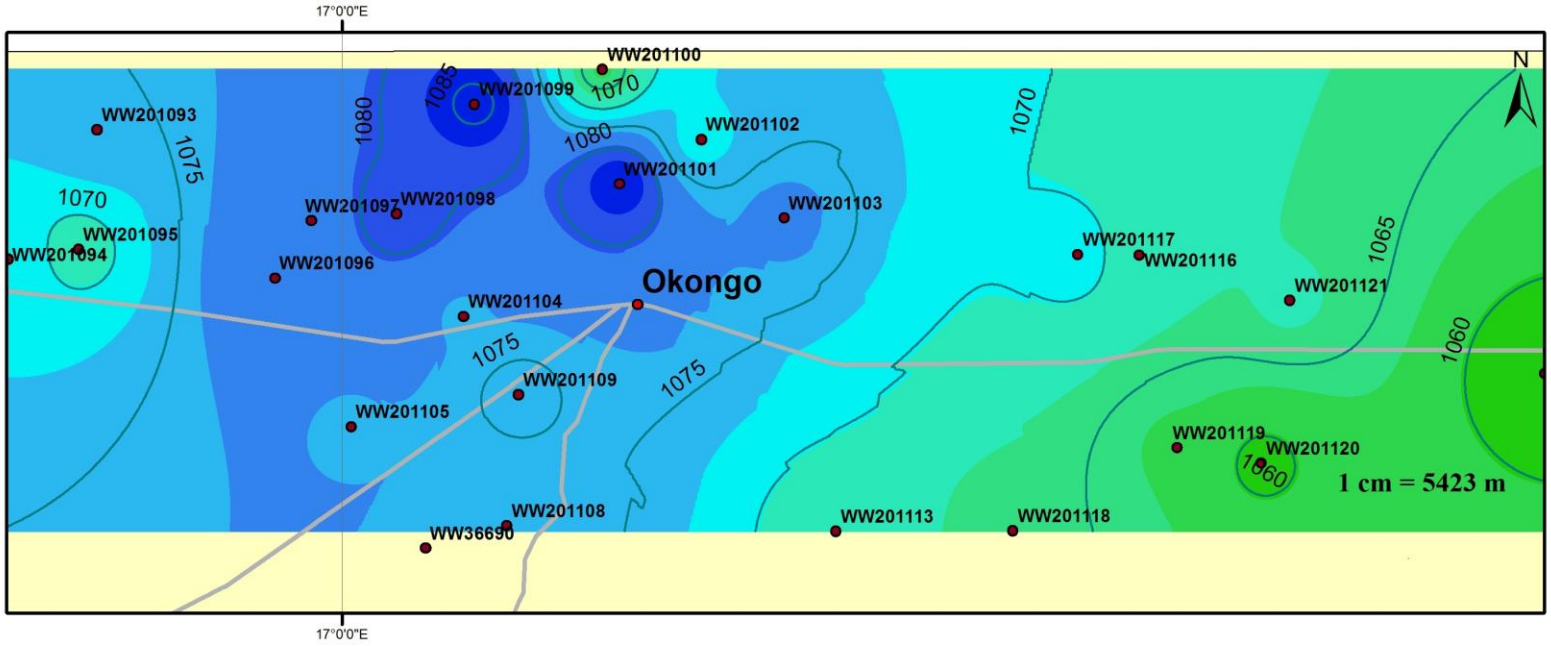

Figure 30. Water table elevation contours for KOH-1 produced with surfer 9 (GoldenSoftware, 2009) and ArcMap 10.1 (Esri, 1999, 2012) bsed on 23 points.

6. Result Interpretation and Discussion

6.1. Overview of the Lithological Data

The results show that the Kalahari Ohangwena Aquifer System is made up of fine to medium sands, silty and clayey sands, clay bands and minor calcrete lenses. Medium to well sorted, fine to medium grained sands make up the groundwater holding bodies. From the surface to several depths medium sorted, fine to medium grained surficial sands of the Kalahari sands occur. Poorly sorted, fine grained silty/clayey sands as well as calcrete lenses separate these surficial sands from medium sorted fine to medium sands. These poorly sorted silty/clayey sands and the calcrete lenses affect vertical groundwater flow and causes perching of groundwater above them and results in the semi-confinement of the medium sorted fine to medium sorted sands below. The perched water bodies form the KOH-0 which is used for water supply by many households in the study area via hand-dug wells. The medium sorted, fine to medium grained sandy layers below make up the semi confined KOH-1.

Besides the hand dug wells, there are currently no boreholes drilled to tap exclusively through the perched KOH-0. However, from the existing borehole lithological data, the thickness of the perched aquifer ranges between 2 and 30 m depending on the surface topography. KOH-1 has an average thickness of 40 m whilst the semi-confining layer (Aquitard) has thicknesses up to >70 m.

6.2. Hydraulic Conductivity and Porosity

The hydraulic conductivity values for the perched aquifer, determined from the different methods used in the study span between 10^{-6} and 10^{-4} m/sec. Hamutoko (2013) computed values of hydraulic conductivity for the perched aquifer that range from 5.98E-05 to 3.35E-04. These are in the same range with those found in this study. A decrease in hydraulic conductivity with depth has been observed from the results with a few distinct layers showing higher values of hydraulic conductivity.

The porosity of KOH-0 materials fall in the range of 0.49 to 16.25%, with lower values encountered at shallow depths and higher values at deeper depths. This means that even though the materials are porous at all depths, the pore spaces are more interconnected at deeper levels. This therefore shows that at shallow depths, only a small number of wells may be placed at a particular site to allow the aquifer to transmit water to these wells. More wells may be placed at deeper levels.

The porosity and hydraulic conductivity results presented here were not analyzed or determined for the same sites, they can therefore not be compared. However, Hamutoko (2013) determined hydraulic conductivity values for the sites where porosity has been computed. A comparison of these two aquifer properties shows no particular trend.

6.3. Analytic Solutions

The groundwater levels recorded in the hand-dug wells and boreholes in the study show a distinct separation between the shallow perched KOH-0 and the semi-confined KOH-1. Groundwater levels in the studied hand-dug wells mirror the topography of the study area

and levels range from <3 m to >16 m. In general, the potentiometric surface of an aquifer is influenced by the surface topography and by surface-water features with the exception of the aquifer being confined (Fetter, 2001). Apart from the ephemeral river beds visible in the study area there are no major surface water features in the study area and the topography is generally uniform. Therefore, no or little influence is expected from either. The near sub-surface water bodies worth noting are those contained in the perched layers north and north-west of Okongo where most hand-dug wells are found. The potentiometric surface of KOH-1 across the study area range from 60-90 m with localized high hydraulic heads (groundwater mount) around the area north and north-west of Okongo, which indicates a groundwater divide in this area. This means that the groundwater contours of KOH-1 in the hand-dug well filled area bend down gradient away from this area. This generally shows that ground waters in the perched KOH-0 may be hydraulically connected to the groundwater table of KOH-1.

The estimated potential amount of flow from KOH-0 to KOH-1 across the aquitard ranges between 2.33E-03 and 5.82E-03 m^3/day. Potentially, between 371 m^3/day and 4370 m^3/day is estimated to flow horizontally within KOH-1 at a given point. The large volume of groundwater flow through KOH-1, relative to the volume seeping through the aquitard, can be attributed to the volume of the aquifer and its higher hydraulic conductivity values. A low volume seeping through the aquitard is to be expected as the lowest hydraulic conductivity values are recorded for this layer.

According to Josef (2015) it takes approximately 1000 years for groundwater to travel through the aquitard from KOH-0 to KOH-1. Also Geyh (1997) determined the ages of

ground waters in the Ohangwena region and found relatively younger C^{14} ages in the area north and north-west of Okongo as compared to other areas in the study area. This area coincides with the area where the water divide or the groundwater mount is observed (see Figure 18 and 31).

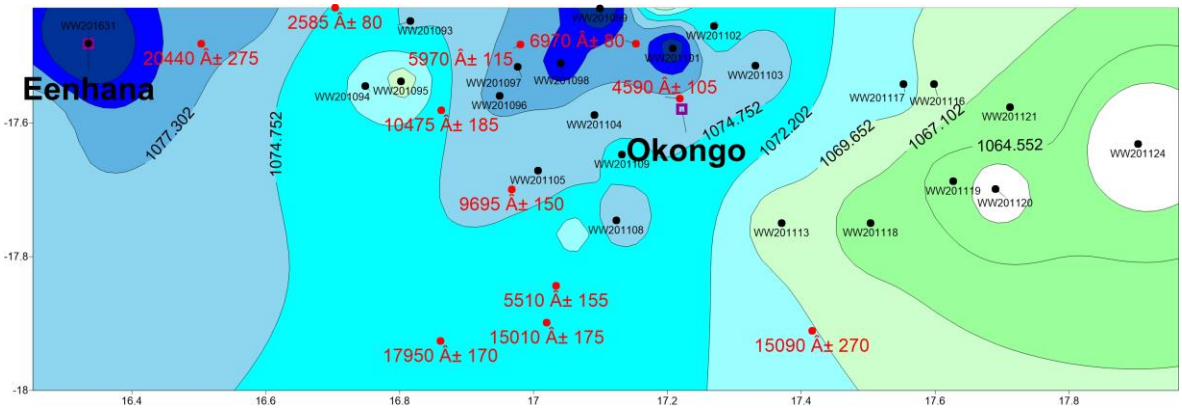

Figure 31. Plot of KOH-1 potentiometric surface with groundwater C-14 ages in years (published in Geyh, 1997); Ages given in red.

Although one may argue that the ground waters are younger in these parts due to the fact that groundwater water recharge in the CEB originate in Angola and flow is directed south-wards towards the Etosha Pan, the position of the groundwater mount and high groundwater gradients relative to the hand dug wells gives an indication that the two aquifers (KOH-0 and KOH-1) may be interacting. This may also be explained by the small amount found to seep through the aquitard as well as the time it takes. However, because the amount of flow within KOH-1 is much larger than that found to flow through the aquitard, the mixing of KOH-0 groundwater with KOH-1 groundwater may be insignificant.

As mentioned earlier, the boreholes used in these simulations are >3 km apart, which means that the values presented in this study, especially those of flow through KOH-1, may be an under estimation of the actual values. The heterogeneous nature of the perched aquifer, aquitard and the semi-confined aquifer were also not taken into account in these calculations. This simplifications could therefore have introduced uncertainties in the obtained values which are not addressed in this study.

7. Conclusions and Recommendations

The purpose of this study was to determine hydraulic parameters for the perched KOH-0 and evaluate its connection to the semi-confined KOH-1. The results contained in this study have shown that the perched aquifer is made up of medium to well sorted, fine to medium grained, porous surficial sands with hydraulic conductivity values that span between 10^{-6} - 10^{-4} m/sec. Through the length of the aquifer, the hydraulic conductivity is higher in some layers and lower in some, this trend is also shown by the porosity.

The results obtained from the employed methods in this study also indicate that KOH-0 is hydraulically connected to KOH-1 and there may therefore be some local recharge into KOH-1 from precipitation in the area. This condition is however only true in areas where the hydraulic gradient of KOH-1 is relatively high. This area coincides with the parts where most hand-dug wells are found.

The results obtained from the different methods in the study will aid in future groundwater development and utilization by means of boreholes. Therefore, to better develop the aquifer for household water supply, the following is recommended:

- Conduct geophysical studies and provide interpretations for the more shallow layers. This would provide a better understanding of the hydrostatigraphy of the area which will in turn allow a better definition of the boundary between the permeable and impermeable layers;

- Set up piezometers in the perched aquifer and monitor the water levels and quality of the water;
- Conduct aquifer tests on the piezometers to further investigate the hydraulic parameters for KOH-0 and the underlying confining layers;
- Bore large diameter wells at selected sites in the study area. These wells are known to operate successfully in low permeability layers due to their ability to draw water from the aquifer even when the pump has ceased to operate. Also, unlike hand dug wells, large diameter bores would be lined and covered in order to prevent seepage of contaminated water from the surface;
- Also, horizontal collector wells that target high permeability layers may be constructed for households in the area. These wells will improve yield and allow maximum amounts of water to be abstracted from identified high hydraulic conductivity layers in the aquifer.

8. References

Alyamani, M.S., and Sen, Z. 1993. *Determination of Hydraulic Conductivity from Grain-Size Distribution Curves. Ground Water*, 31,551-555.

Amutenya, D.P.K., 2011. *Fluoride distribution in Namibia's Groundwater and identification of possible sources Unpublished Honours thesis*, University of Namibia.

Ananias, A.L., 2012. *An estimation of the transmissivity of Ohangwena I and II Aquifers Unpublished Honours thesis*, University of Namibia.

Behera, S., Jha, M.K., Kar, S. 2003. *Dynamics of water flow and fertilizer solute leaching in lateritic soils of Kharagpur region, India. Agricultural Water Management.* 63(2), p.77-98.

Bittner, A., 2006. *Desk Study Report: Cuvelai - Etosha Groundwater Investigatiion*. Bittner Water Consult.

Christelis et al., 2001. *Groundwater in Namibia. An explanation of the Hydrogeological Map. John Meinert Printing*.

Carman, P.C., 1956. *Flow of Gases through Porous Media*. Butterworths Scientific Publications, London.

Cherry, J.A., Parker, B.L., Bradbury, K.R., Eaton, T.T., Gorkowitz, M.G., Hart, D.J., and Borchardt, M.A., 2004. *Role of Aquitards in the Protection of Aquifers from Contamination: A "State of Science" Report.* Awwa Research Foundation.

Cozzarelli, I.M., Herman, J.S., Baedecker, M.J. Fischer, J.M., 1999. *Geochemical heterogeneity of a gasoline-contaminated aquifer. Journal of Contaminant Hydrology*. 40 (3), pp.261-284.

Darcy, H., 1856. *Les fountaines publiques de la Ville de Dijon*, Victor Dalmont, Paris.

Esri, 1999, 2012. *ArcMap10.1.* GIS software. http://www.esri.com.

Fetter, C.W., 2001. *Applied Hydrogeology. 4th Edition ed.* New Jersey: Prentice Hall.

Fitts, G.R., 2002. *Groundwater Science.* Academic Press, UK.

Freeze, R.A. and Cherry, J.A., 1979. *Groundwater*. Prentice Hall Inc.

Goldensoftware Inc., 1993-2009. *Surfer 9.8.669. Surface Mapping System.* http://www.goldensoftware.com.

Golder Associates, 2005. *Approaches and Methods for Evaluation Vertical Transport in Groundwater-Hydrogeological Assessment Tools Project.* 05-1412-058.

Hamutoko, J., 2013. *Estimation of Groundwater Vulnerability to Pollution based on DRASTIC and BTU method in the upper Cuvelai-Etosha basin, Namibia*. Unpublished Master thesis.

Hazen, A., 1892. *Some Physical Properties of Sands and Gravels, with Special Reference to their Use in Filtration*. 24th Annual Report, Massachusetts State Board of Health, Pub.Doc. No.34, 539-556.

Hiscock, K.M., 2005. *Hydrogeology: Principles and Practice*. Oxford (Blackwell Publishing).

Kozeny, J., 1927. *Uber Kapillare Leitung Des Wassers in Boden. Sitzungsber Akad. Wiss. Wien Math. Naturwiss*. Kl, Abt. 2a, 136, 271-306 (In German).

Kruseman, G.P and de Ridder, N.A., 1990. *Analysis and Evaluation of Pumping Test Data*, 2nd edition.

Lappala, E.G., 1978. *Quantitative Hydrogeology of the Upper Republican Natural Resources District, South West Nebraska, U.S.* Geological Survey: Water Resources Investigations 78-38.

Lohe, C., Lindenmeir, F., and Miller, R.M.G., 2013. *Drill-Log Interpretation and Evaluation of Drillings KOH I and KOH II Aquifer, Ohangwena Region, Cuvelai-Etosha Basin.* BGR, Technical Note No.1.

Mendelsohn, J.E., Obeid, S. and Roberts, C., 2000. *A profile of northcentral Namibia*. (Gamsberg Macmillan), Windhoek.

Miller, R.M.G., 1997. *The Owambo Basin of Northern Namibia. In R. Selly, African Basins, Sedimentary Basins of the World* (pp. 237-268). Amsterdam: Elsevier Science B.V.

Miller, R.M.G., 2008. *The Geology of Namibia: Kalahari Group*. Volume 3.24.

Miller, R. M., Pickford, M., & Senut, B., 2010. *The Geology, Palaeontology and Evolution of the Etosha Pan, Namibia: Implications for Terminal Kalahari Deposition*. South African Journal of Geology, 113(3), 307-334.

Moench, A.F., 1997. *Flow to a well of finite diameter in a homogeneous, anisotropic water-table aquifer, Water Resources Research*, vol. 33, no. 6, pp. 1397-1407.

Nakwafila, A., 2011: *Water quality of hand dug wells in 5 example regions of Namibia*. BSc (honours) thesis, University of Namibia.

Neuman, S.P., 1974. *Effect of partial penetration on flow in unconfined aquifers considering delayed gravity response, Water Resources Research*, vol. 10, no. 2, pp. 303-312.

Petrus, I.N., 2011. *Factors affecting Fluoride concentration in groundwater in the Cuvelai-Etosha Basin and testing of the available lab scale defluoridation technique*. Unpublished Honours Thesis, University of Namibia.

Reichard, E.G., Izbicki, J.A., Martin, P. 1995. *Implications of uncertainty in exposure assessment for groundwater contamination. Proceeding from the Rome Symposium, September 1994, Assessing and Managing Health Risks from Drinking Water Contamination: Approaches and Applications.* IAHS Publ. no 235, pp. 211-219.

Rushton, K.R., 2003. *Groundwater Hydrology: Conceptual and Computational Models.* John Wiley & Sons Ltd. ISBN: 0-470-85004-3.

Saxton, K. E. 2013, 2005, 2003. *USDA Agricultural Research Service.* Retrieved from http://http//hydrolab.arsusda.gov/SPAW/Index.htm.

Shepherd, R.G. 1989. *Correlations of Permeability and Grain Size. Groundwater*. 27(5): 663-638.

Stibinger, J., 2014. *Examples of Determining the Hydraulic Conductivity of Soils: Theory and Applications of Selected Basic Methods. University Handbook on Soil Hydraulics.* Jan Evangelista Purkyně University, Faculty of the Environment. ISBN 978-80-7414-836-1 (online: pdf).

Tartakovsky, G.D., and Neuman, S.P., 2007. *Three-dimensional saturated-unsaturated flow with axial symmetry to a partially penetrating well in a compressible unconfined aquifer, Water Resources Research*, W01410, doi: 1029/2006WR005153.

Thangarajan et al., 2007. *Groundwater: Resource Resource Evaluation, Augmentation, Contamination, Restoration, Modelling and Management*. Capital Publishing Company, India.

van Wyk, B., 2009. *Groundwater Investigation of the Cuvelai-Etosha Basin*. Tech. rept. BGR internal document.

Vukovic, M., and Soro, A., 1992. *Determination of Hydraulic Conductivity of Porous Media from Grain-Size Composition*. Water Resources Publications, Littleton, Colorado.

Walzer, A., 2010. *Multi-Layered Aquifers in the Central-North of Namibia and their Potential Use for Water Supply*.

Wurdac, S., 2008. *Hydrogeological and hydrochemical investigations in rural areas of north-central Namibia*.

Appendices

Appendix A

Table 5. KOH-0 and aquitard textures (abbreviations explained under list of abbreviations)

WW #	Latitude	Longitude	KOH-0 thickness (m)	KOH-0 texture	Aquitard texture
200470	-17.64003	17.74989	32	med sorted , sub-well round fs + minor silt	none
200471	-17.64032	17.71146	12	med sorted fs-ms, sub-well	none
200474	-17.68165	17.65702	15	med sorted fs-ms, sub-well	Poorly sorted fs with silt
200482	-17.67204	17.79879	3	med sorted fs-ms, sub-well	Calcrete
200656	-18.37430	17.9346	5	med sorted fs-cs, sub-well	Clayey sand
201098	-17.51112	17.04054	22	med sorted, ms	Poorly sorted fs-ms with silt
201100	-17.40259	17.19537	3	med sorted, ms	Calcrete
201102	-17.45513	17.26945	5	med sorted, fs	Poorly sorted fs with silt
201103	-17.51449	17.33179	4	med sorted, fs	Poorly sorted fs with silt
201104	-17.58844	17.09107	4	med sorted, fs	Poorly sorted fs with silt
201105	-17.67141	17.00655	5	med sorted, fs	Poorly sorted fs with silt
201109	-17.64738	17.13229	15	med sorted, ms	Poorly sorted fs with silt
201112	-17.68846	17.35354	16	med sorted, ms	Calcrete
201114	-17.74996	17.37082	6	med sorted, ms	Poorly sorted fs with silt
201124	-17.63169	17.90321	20	med sorted, fs-ms	Poorly sorted fs with silt
201631	-17.48100	16.33518	10	med-well sorted fs-ms	Poorly sorted fs-ms
201632	-17.48124	16.33517	10	med-well sorted fs + minor silt	Poorly sorted fs-ms
201634	-17.45247	16.11419	6	med sorted fs-cs	Sandy clay
201635	-17.39487	16.43557	5	med sorted, sub-well rounded fs	Clayey sand
201636	-17.55015	16.67453	14	poor-med sorted fs-ms	Clayey sand
201637	-17.73995	16.67805	8	med sorted fs-ms	Clayey sand

Table 6. Minimum KOH-0 hydraulic conductivity estimates from texture and degree of sorting

BH #	Latitude	Longitude	Aquifer thickness (m)	Estimated Kf (m/sec)
WW200470	-17.64003	17.74989	32	1.20E-04
WW200471	-17.64032	17.71146	12	2.11E-04
WW200474	-17.68165	17.65702	15	2.11E-04
WW200482	-17.67204	17.79879	3	2.11E-04
WW200656	-18.37430	17.9346	5	2.41E-04
WW201098	-17.51112	17.04054	22	2.85E-04
WW201100	-17.40259	17.19537	3	2.85E-04
WW201102	-17.45513	17.26945	5	1.27E-04
WW201103	-17.51449	17.33179	4	1.27E-04
WW201104	-17.58844	17.09107	4	1.27E-04
WW201105	-17.67141	17.00655	5	1.27E-04
WW201109	-17.64738	17.13229	15	2.85E-04
WW201112	-17.68846	17.35354	16	2.85E-04
WW201114	-17.74996	17.37082	6	2.85E-04
WW201124	-17.63169	17.90321	20	2.22E-04
WW201631	-17.48100	16.33518	10	2.22E-04
WW201632	-17.48124	16.33517	10	1.27E-04
WW201634	-17.45247	16.11419	6	2.54E-04
WW201635	-17.39487	16.43557	5	1.20E-04
WW201636	-17.55015	16.67453	14	2.06E-04
WW201637	-17.73995	16.67805	8	2.22E-04

Table 7. Minimum aquitard hydraulic conductivities estimated from texture and degree of sorting

BH #	Latitude	Longitude	Aquitard texture	Kf (m/sec)
WW200470	-17.64003	17.74989	none	-
WW200471	-17.64032	17.71146	none	-
WW200474	-17.68165	17.65702	Poorly sorted fine grained sand with silt	1.27E-04
WW200482	-17.67204	17.79879	Calcrete	3.17E-09
WW200656	-18.37430	17.9346	Clayey sand	2.45E-06

BH #	Latitude	Longitude	Aquitard texture	Kf (m/sec)
WW201098	-17.51112	17.04054	Poorly sorted fine grained sand with silt	1.59E-04
WW201100	-17.40259	17.19537	Calcrete	3.17E-09
WW201102	-17.45513	17.26945	Poorly sorted fine grained sand with silt	1.27E-04
WW201103	-17.51449	17.33179	Poorly sorted fine grained sand with silt	1.27E-04
WW201104	-17.58844	17.09107	Poorly sorted fine grained sand with silt	1.27E-04
WW201105	-17.67141	17.00655	Poorly sorted fine grained sand with silt	1.27E-04
WW201109	-17.64738	17.13229	Poorly sorted fine grained sand with silt	1.27E-04
WW201112	-17.68846	17.35354	Calcrete	3.17E-09
WW201114	-17.74996	17.37082	Poorly sorted fine grained sand with silt	1.27E-04
WW201124	-17.63169	17.90321	Poorly sorted fine grained sand with silt	1.27E-04
WW201631	-17.48100	16.33518	Poorly sorted fine to medium grained sand	1.90E-04
WW201632	-17.48124	16.33517	Poorly sorted fine to medium grained sand	1.90E-04
WW201634	-17.45247	16.11419	Sandy clay	2.17E-06
WW201635	-17.39487	16.43557	Clayey sand	2.45E-06
WW201636	-17.55015	16.67453	Clayey sand	2.45E-06
WW201637	-17.73995	16.67805	Clayey sand	2.45E-06

Appendix B Grain Size Distribution

a. Eenhana Forest Site

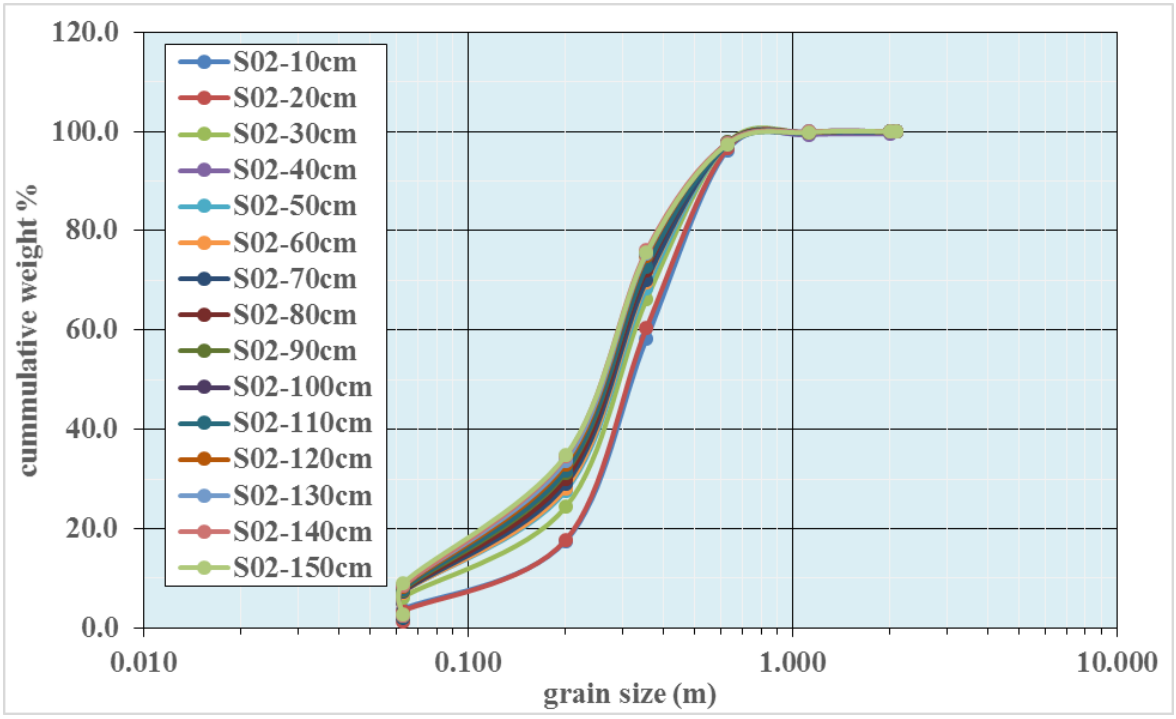

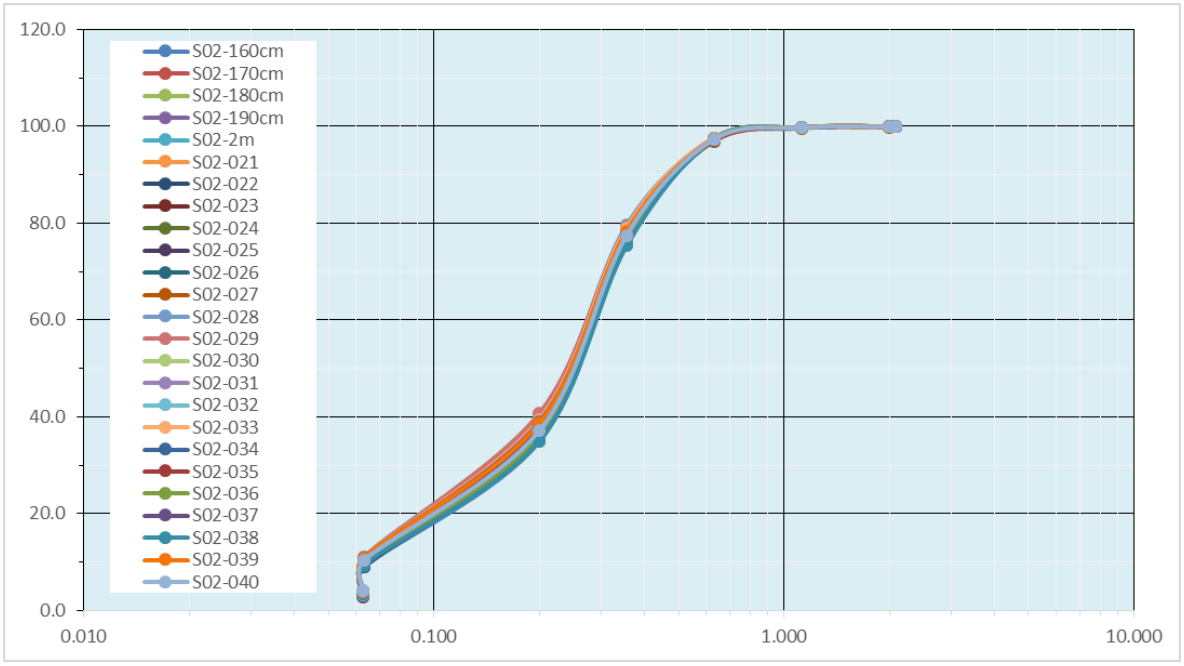

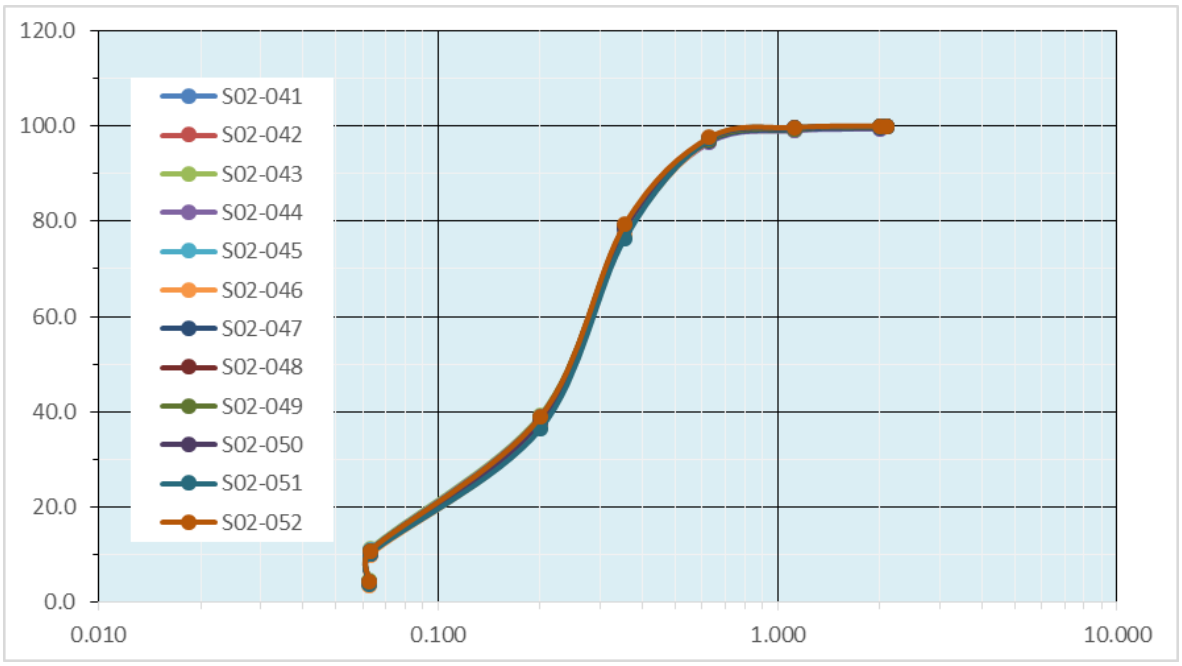
120.0
100.0
80.0
60.0
40.0
20.0
0.0
0.010
0.100
1.000
10.000
S02-041
S02-042
S02-043
S02-044
S02-045
S02-046
S02-047
S02-048
S02-049
S02-050
S02-051
S02-052

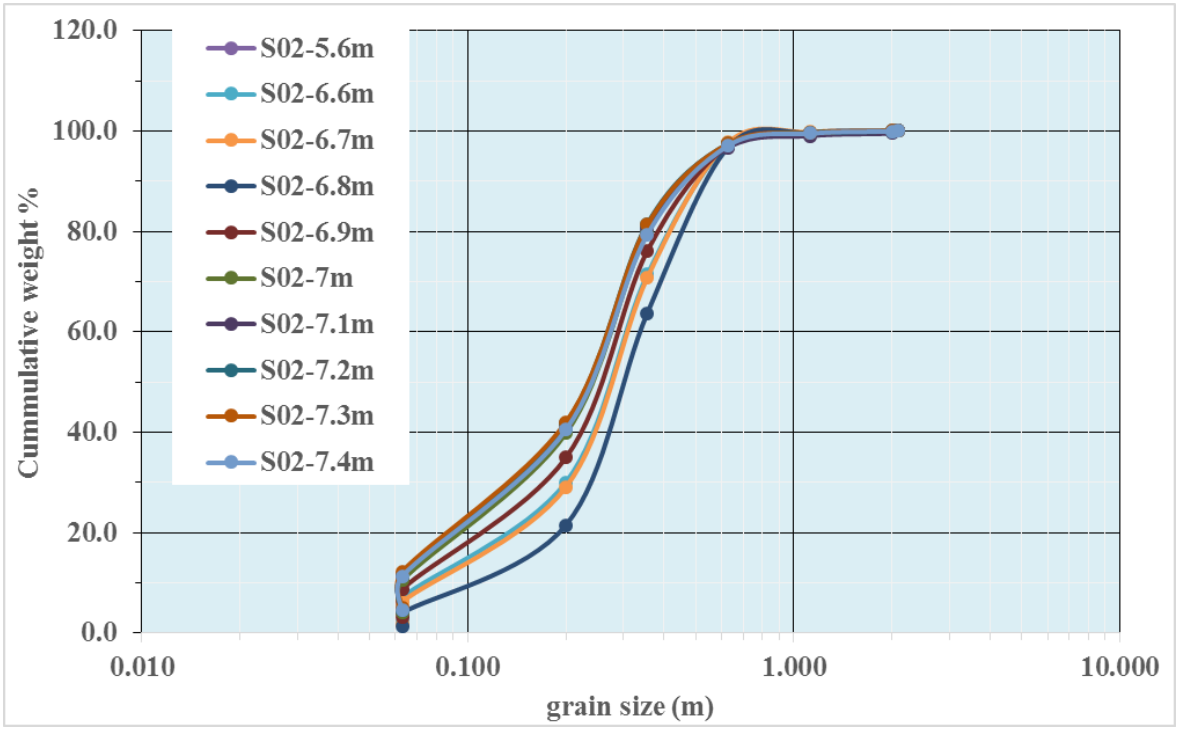
Cummulative weight %
120.0
100.0
80.0
60.0
40.0
20.0
0.0
0.010
0.100
1.000
10.000
grain size (m)
S02-5.6m
S02-6.6m
S02-6.7m
S02-6.8m
S02-6.9m
S02-7m
S02-7.1m
S02-7.2m
S02-7.3m
S02-7.4m

Table 8. Hydraulic conductivity calculations from grain size distribution curves for Eenhana Forest Site

Sample#	d60	d10	U(d60/d10)	K (m/s)	K (m/d)
S02-10cm	0.35	0.140	2.500	1.95E-04	16.84
S02-20cm	0.35	0.140	2.500	1.95E-04	16.84
S02-30cm	0.32	0.085	3.765	6.61E-05	5.71
S02-40cm	0.31	0.071	4.366	4.47E-05	3.86
S02-50cm	0.31	0.071	4.366	4.47E-05	3.86
S02-60cm	0.31	0.071	4.366	4.47E-05	3.86
S02-70cm	0.31	0.071	4.366	4.47E-05	3.86
S02-80cm	0.3	0.070	4.286	4.36E-05	3.77
S02-90cm	0.3	0.070	4.286	4.36E-05	3.77
S02-100cm	0.3	0.070	4.286	4.36E-05	3.77
S02-110cm	0.3	0.070	4.286	4.36E-05	3.77
S02-120cm	0.3	0.065	4.615	3.70E-05	3.20
S02-130cm	0.3	0.065	4.615	3.70E-05	3.20
S02-140cm	0.3	0.065	4.615	3.70E-05	3.20
S02-150cm	0.3	0.065	4.615	3.70E-05	3.20
S02-160cm	0.295	0.065	4.538	3.72E-05	3.21
S02-170cm	0.295	0.065	4.538	3.72E-05	3.21
S02-180cm	0.295	0.065	4.538	3.72E-05	3.21
S02-190cm	0.295	0.065	4.538	3.72E-05	3.21
S02-2m	0.294	0.065	4.523	3.72E-05	3.21
S02-021	0.294	0.065	4.523	3.72E-05	3.21
S02-022	0.294	0.065	4.523	3.72E-05	3.21
S02-023	0.294	0.065	4.523	3.72E-05	3.21
S02-024	0.29	0.061	4.754	3.24E-05	2.80
S02-025	0.29	0.061	4.754	3.24E-05	2.80
S02-026	0.29	0.061	4.754	3.24E-05	2.80
S02-027	0.29	0.061	4.754	3.24E-05	2.80
S02-028	0.29	0.061	4.754	3.24E-05	2.80
S02-029	0.29	0.061	4.754	3.24E-05	2.80
S02-030	0.29	0.061	4.754	3.24E-05	2.80
S02-031	0.29	0.061	4.754	3.24E-05	2.80
S02-032	0.295	0.061	4.836	3.23E-05	2.79
S02-033	0.29	0.061	4.754	3.24E-05	2.80
S02-034	0.29	0.061	4.754	3.24E-05	2.80

Sample#	d60	d10	U(d60/d10)	K (m/s)	K (m/d)
S02-035	0.29	0.061	4.754	3.24E-05	2.80
S02-036	0.29	0.061	4.754	3.24E-05	2.80
S02-037	0.29	0.061	4.754	3.24E-05	2.80
S02-038	0.295	0.061	4.836	3.23E-05	2.79
S02-039	0.29	0.061	4.754	3.24E-05	2.80
S02-040	0.299	0.061	4.902	3.22E-05	2.78
S02-041	0.29	0.061	4.754	3.24E-05	2.80
S02-042	0.29	0.061	4.754	3.24E-05	2.80
S02-043	0.29	0.061	4.754	3.24E-05	2.80
S02-044	0.29	0.061	4.754	3.24E-05	2.80
S02-045	0.29	0.061	4.754	3.24E-05	2.80
S02-046	0.299	0.061	4.902	3.22E-05	2.78
S02-047	0.299	0.061	4.902	3.22E-05	2.78
S02-048	0.299	0.061	4.902	3.22E-05	2.78
S02-049	0.299	0.061	4.902	3.22E-05	2.78
S02-050	0.299	0.061	4.902	3.22E-05	2.78
S02-051	0.299	0.061	4.902	3.22E-05	2.78
S02-052	0.299	0.061	4.902	3.22E-05	2.78
S02-053	0.28	0.061	4.590	3.27E-05	2.82
S02-054	0.28	0.061	4.590	3.27E-05	2.82
S02-055	0.28	0.061	4.590	3.27E-05	2.82
S02-5.6m	0.28	0.061	4.590	3.27E-05	2.82
S02-6.6m	0.31	0.075	4.133	5.04E-05	4.36
S02-6.7m	0.31	0.080	3.875	5.82E-05	5.03
S02-6.8m	0.34	0.110	3.091	1.15E-04	9.95
S02-6.9m	0.29	0.065	4.462	3.73E-05	3.22
S02-7m	0.289	0.061	4.738	3.24E-05	2.80
S02-7.1m	0.289	0.061	4.738	3.24E-05	2.80
S02-7.2m	0.289	0.061	4.738	3.24E-05	2.80
S02-7.3m	0.289	0.061	4.738	3.24E-05	2.80
S02-7.4m	0.289	0.061	4.738	3.24E-05	2.80

b. Ephemeral River

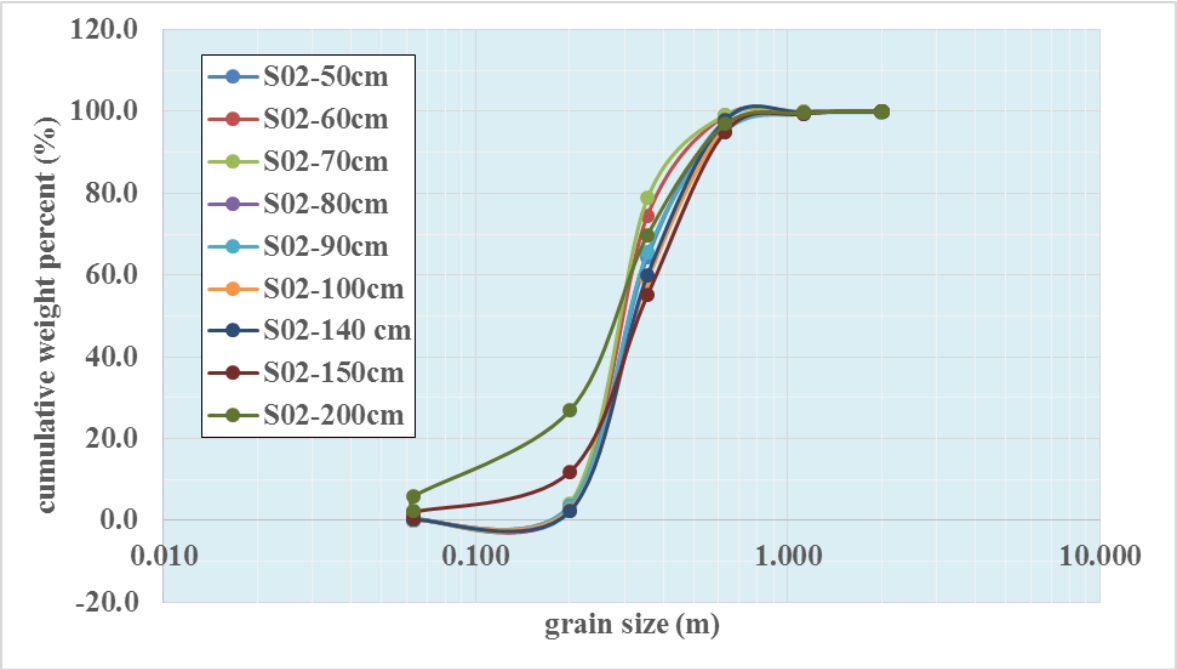

Table 9. Hydraulic conductivity estimates of KOH-0 material based on grain size distribution at Ephemeral River

sample #	d60	d10	U(d60/d10)	K (m/s)	K (m/d)
S02-50cm	0.35	0.23	1.52173913	0.00058	50.3193
S02-60cm	0.32	0.23	1.391304348	0.00059	51.2531
S02-70cm	0.31	0.23	1.347826087	0.0006	51.5881
S02-80cm	0.35	0.23	1.52173913	0.00058	50.3193
S02-90cm	0.355	0.245	1.448979592	0.00067	57.6736
S02-100cm	0.355	0.245	1.448979592	0.00067	57.6736
S02-140 cm	0.355	0.245	1.448979592	0.00067	57.6736
S02-150cm	0.399	0.199	2.005025126	0.00041	35.5964
S02-200cm	0.31	0.08	3.875	5.8E-05	5.0253

c. Oshandi

Table 10. Estimated values of Hydraulic conductivity of material from Oshandi site based on SPAW

sample depth (m)	Silt + clay (g)	clay (g)	% clay	% silt	% sand	Textural class	SPAW sat. Hydraulic cond. (mm/hr)	K (m/s)	K (m/day)
1	0.164	0.013	1.30	15.10	83.60	loamy sand	102.42	2.85E-04	2.46
2	0.2	0.046	4.60	15.40	80.00	loamy sand	96.74	2.69E-04	2.32
3	0.241	0.006	0.60	23.50	75.90	loamy sand	91.16	2.53E-04	2.19
4	0.138	0.027	2.70	11.09	86.21	loamy sand	125.79	3.49E-04	3.02
5	0.1611	0.063	6.30	9.81	83.89	loamy sand	93.86	2.61E-04	2.25
6	0.1713	0.0761	7.60	9.51	82.90	loamy sand	77.73	2.16E-04	1.87
7	0.2201	0.0709	7.08	14.90	78.02	loamy sand	79.03	2.20E-04	1.90
8	0.1502	0.081	8.09	6.91	85.00	loamy sand	79.87	2.22E-04	1.92
9	0.105	0.0907	9.03	1.42	89.55	sand	85.3	2.37E-04	2.05
10	0.099	0.0603	6.02	3.86	90.11	sand	101.77	2.83E-04	2.44
11	0.21	0.067	6.69	14.27	79.04	loamy sand	80.18	2.23E-04	1.92
12	0.25	0.0943	9.42	15.55	75.04	sandy loam	63.65	1.77E-04	1.53
13	0.121	0.0614	6.12	5.94	87.95	loamy sand	99.12	2.75E-04	2.38
14	0.19	0.0972	9.72	9.28	81.01	loamy sand	63.38	1.76E-04	1.52
15	0.112	0.093	9.27	1.89	88.84	loamy sand	77.01	2.14E-04	1.85

sample depth (m)	Silt + clay (g)	clay (g)	% clay	% silt	% sand	Textural class	SPAW sat. Hydraulic cond. (mm/hr)	K (m/s)	K (m/day)
16	0.113	0.073	7.30	4.00	88.70	loamy sand	91.99	2.56E-04	2.21
17	0.141	0.0433	4.32	9.74	85.94	loamy sand	115.01	3.19E-04	2.76
18	0.22	0.0654	0.07	0.15	99.78	sand	115.01	3.19E-04	2.76
19	0.082	0.0499	4.97	3.20	91.84	sand	112.58	3.13E-04	2.70
20	0.113	0.0588	5.87	5.41	88.72	sand	108.2	3.01E-04	2.60
21	0.0699	0.0837	8.23	1.36	90.41	sand	85.3	2.37E-04	2.05
22	0.055	0.071	7.05	1.59	91.36	sand	94.41	2.62E-04	2.27
23	0.0526	0.0673	6.71	1.47	91.82	sand	103.11	2.86E-04	2.47
24	0.0428	0.0814	8.10	3.84	88.05	loamy sand	83.12	2.31E-04	1.99
25	0.0729	0.0622	6.20	1.07	92.73	sand	104.44	2.90E-04	2.51
26	0.2684	0.0283	2.82	23.90	73.28	loamy sand	113.69	3.16E-04	2.73
27	0.3207	0.0798	7.96	24.04	67.99	sandy loam	66.81	1.86E-04	1.60
28	0.3482	0.052	5.19	29.56	65.25	sandy loam	76.49	2.12E-04	1.84
29	0.3285	0.0319	3.19	29.62	67.20	sandy loam	94.06	2.61E-04	2.26
30	0.3463	0.0293	2.93	31.65	65.42	sandy loam	99.54	2.77E-04	2.39

d. Summary of hydraulic conductivity estimates for soil samples calculated using four different methods.

Table 11. Hydraulic conductivity estimates for soil materials determined using four different methods

sample depth (m)	Kf (m/sec)					
	Sieving - UNAM	CAMSIZER-GERMANY				Sedimentation
	BEYER	HAZEN	SEELHEIM	BIALAS	BEYER	SPAW
Eenhana Forest site						
0.1	2.03E-06	2.76E-04	3.26E-04	8.78E-05	1.95E-04	
0.2	2.07E-06	2.81E-04	3.13E-04	8.64E-05	1.95E-04	
0.3	2.01E-06	2.03E-04	2.69E-04	6.44E-05	6.61E-05	
0.4	2.00E-06	1.72E-04	2.37E-04	5.37E-05	4.47E-05	
0.5	2.03E-06	1.80E-04	2.47E-04	5.63E-05	4.47E-05	
0.6	2.03E-06	1.81E-04	2.41E-04	5.58E-05	4.47E-05	
0.7	2.03E-06	1.77E-04	2.36E-04	5.41E-05	4.47E-05	
0.8	2.17E-06	1.70E-04	2.25E-04	5.20E-05	4.36E-05	
0.9	2.16E-06	1.68E-04	2.17E-04	5.04E-05	4.36E-05	
1	2.17E-06	1.62E-04	2.11E-04	4.84E-05	4.36E-05	
1.1	2.17E-06	1.64E-04	2.15E-04	4.96E-05	4.36E-05	
1.2	2.11E-06	1.59E-04	2.04E-04	4.76E-05	3.70E-05	
1.3	2.11E-06	1.55E-04	2.00E-04	4.65E-05	3.70E-05	
1.4	2.14E-06	1.55E-04	1.96E-04	4.58E-05	3.70E-05	
1.5	2.16E-06	1.49E-04	1.96E-04	4.51E-05	3.70E-05	
1.6		1.50E-04	1.94E-04	4.51E-05	3.72E-05	
1.7		1.48E-04	1.89E-04	4.44E-05	3.72E-05	
1.8		1.41E-04	1.85E-04	4.30E-05	3.72E-05	
1.9		1.47E-04	1.88E-04	4.40E-05	3.72E-05	
2		1.43E-04	1.84E-04	4.30E-05	3.72E-05	
2.1		1.44E-04	1.83E-04	4.30E-05	3.72E-05	

sample depth (m)	Kf (m/sec)					
	Sieving - UNAM	CAMSIZER-GERMANY				Sedimentation
	BEYER	HAZEN	SEELHEIM	BIALAS	BEYER	SPAW
2.2		1.49E-04	1.89E-04	4.44E-05	3.72E-05	
2.3		1.39E-04	1.76E-04	4.20E-05	3.72E-05	
2.4		1.37E-04	1.74E-04	4.13E-05	3.24E-05	
2.5		1.31E-04	1.70E-04	3.97E-05	3.24E-05	
2.6		1.33E-04	1.76E-04	4.10E-05	3.24E-05	
2.7		1.26E-04	1.73E-04	3.94E-05	3.24E-05	
2.8		1.27E-04	1.65E-04	3.84E-05	3.24E-05	
2.9		1.29E-04	1.65E-04	3.84E-05	3.24E-05	
3		1.31E-04	1.72E-04	4.00E-05	3.24E-05	
3.1		1.33E-04	1.73E-04	4.06E-05	3.24E-05	
3.2		1.43E-04	1.88E-04	4.33E-05	3.23E-05	
3.3		1.28E-04	1.70E-04	3.94E-05	3.24E-05	
3.4		1.32E-04	1.76E-04	4.06E-05	3.24E-05	
3.5		1.32E-04	1.76E-04	4.03E-05	3.24E-05	
3.6		1.41E-04	1.89E-04	4.33E-05	3.24E-05	
3.7		1.29E-04	1.74E-04	3.97E-05	3.24E-05	
3.8		1.46E-04	1.94E-04	4.47E-05	3.23E-05	
3.9		1.28E-04	1.75E-04	3.97E-05	3.24E-05	
4		1.34E-04	1.81E-04	4.20E-05	3.22E-05	
4.1		1.32E-04	1.80E-04	4.16E-05	3.24E-05	
4.2		1.29E-04	1.75E-04	4.00E-05	3.24E-05	
4.3		1.24E-04	1.73E-04	3.91E-05	3.24E-05	
4.4		1.27E-04	1.74E-04	3.97E-05	3.24E-05	
4.5		1.27E-04	1.74E-04	3.97E-05	3.24E-05	

sample depth (m)	Kf (m/sec)					
	Sieving - UNAM	CAMSIZER-GERMANY				Sedimentation
	BEYER	HAZEN	SEELHEIM	BIALAS	BEYER	SPAW
4.6		1.40E-04	1.85E-04	4.30E-05	3.22E-05	
4.7		1.31E-04	1.74E-04	4.03E-05	3.22E-05	
4.8		1.30E-04	1.74E-04	4.03E-05	3.22E-05	
4.9		1.29E-04	1.74E-04	4.03E-05	3.22E-05	
5		1.35E-04	1.78E-04	4.20E-05	3.22E-05	
5.1		1.37E-04	1.88E-04	4.26E-05	3.22E-05	
5.2		1.29E-04	1.73E-04	4.00E-05	3.22E-05	
5.3		1.29E-04	1.68E-04	3.91E-05	3.27E-05	
5.4		1.25E-04	1.66E-04	3.81E-05	3.27E-05	
5.5		1.28E-04	1.66E-04	3.88E-05	3.27E-05	
5.6		1.25E-04	1.65E-04	3.81E-05	3.27E-05	
6.6		1.77E-04	2.26E-04	5.24E-05	5.04E-05	
6.7		1.88E-04	2.31E-04	5.50E-05	5.82E-05	
6.8		2.47E-04	2.86E-04	7.32E-05	1.15E-04	
6.9		1.52E-04	1.92E-04	4.58E-05	3.73E-05	
7		1.32E-04	1.68E-04	3.97E-05	3.24E-05	
7.1		1.21E-04	1.60E-04	3.69E-05	3.24E-05	
7.2		1.19E-04	1.59E-04	3.67E-05	3.24E-05	
7.3		1.15E-04	1.58E-04	3.55E-05	3.24E-05	
7.4		1.23E-04	1.66E-04	3.78E-05	3.24E-05	
Ephemeral River between Eenhana and Okongo						
0.5		6.0E-04	3.3E-04	1.5E-04	5.82E-04	
0.6		5.6E-04	2.9E-04	1.3E-04	5.93E-04	
0.7		5.1E-04	2.7E-04	1.2E-04	5.97E-04	

sample depth (m)	Kf (m/sec)					
	Sieving - UNAM	CAMSIZER-GERMANY				Sedimentation
	BEYER	HAZEN	SEELHEIM	BIALAS	BEYER	SPAW
0.8		5.5E-04	3.1E-04	1.3E-04	5.82E-04	
0.9		5.3E-04	3.0E-04	1.3E-04	6.68E-04	
1		5.7E-04	3.4E-04	1.4E-04	6.68E-04	
1.4		6.2E-04	3.5E-04	1.6E-04	6.68E-04	
1.5		3.7E-04	3.5E-04	1.2E-04	4.12E-04	
2		2.0E-04	2.4E-04	6.0E-05	5.82E-04	
Oshandi Deep borehole						
1						2.85E-04
2						2.69E-04
3						2.53E-04
4						3.49E-04
5						2.61E-04
6						2.16E-04
7						2.20E-04
8						2.22E-04
9						2.37E-04
10						2.83E-04
11						2.23E-04
12						1.77E-04
13						2.75E-04
14						1.76E-04
15						2.14E-04
16						2.56E-04
17						3.19E-04

sample depth (m)	Kf (m/sec)					
	Sieving - UNAM	CAMSIZER-GERMANY				Sedimentation
	BEYER	HAZEN	SEELHEIM	BIALAS	BEYER	SPAW
18						3.19E-04
19						3.13E-04
20						3.01E-04
21						2.37E-04
22						2.62E-04
23						2.86E-04
24						2.31E-04
25						2.90E-04
26						3.16E-04
27						1.86E-04
28						2.12E-04
29						2.61E-04
30						2.77E-04

Appendix C. Standard Hydraulic Conductivity values for known geological materials

Material	K(cm/sec)	Source
Gravel	10^{-1} to 100	1
Clean sand	10^{-4} to 1	1
Silty sand	10^{-5} to 10^{-1}	1
Silt	10^{-7} to 10^{-3}	1
Glacial till	10^{-10} to 10^{-4}	1
Clay	10^{-10} to 10^{-6}	1,2
Limestone and dolomite	10^{-7} to 1	1
Fractured basalt	10^{-5} to 1	1
Sandstone	10^{-8} to 10^{-3}	1
Igneous and metamorphic rock	10^{-11} to 10^{-2}	1
Shale	10^{-14} to 10^{-8}	2

Figure 32. Range of Saturated Hydraulic conductivities for various geological materials (source: Fitts, 2002 after Cherry, 1979).

Grain-Size Class or Range From Sample Description	Degree of Sorting			Silt Content		
	Poor	Moderate	Well	Slight	Moderate	High
Fine-Grained Materials						
Clay	Less than .001					
Silt, clayey	1 - 4					
Silt, slightly sandy	5					
Silt, moderately sandy	7 - 8					
Silt, very sandy	9 - 11					
Sandy silt	11					
Silty sand	13					
Sands and gravels(1)						
Very fine sand	13	20	27	23	19	13
Very fine to fine sand	27	27	-	24	20	13
Very fine to medium sand	36	41-47	-	32	27	21
Very fine to coarse sand	48	-	-	40	31	24
Very fine to very coarse sand	59	-	-	51	40	29
Very fine sand to fine gravel	76	-	-	67	52	38
Very fine sand to medium gravel	99	-	-	80	66	49
Very fine sand to coarse gravel	128	-	-	107	86	64
Fine sand	27	40	53	33	27	20
Fine to medium sand	53	67		48	39	30
Fine to coarse sand	57	65-72	-	53	43	32
Fine to very coarse sand	70	-	-	60	47	35
Fine sand to fine gravel	88	-	-	74	59	44
Fine sand to medium gravel	114	-	-	94	75	57
Fine sand to coarse gravel	145	-	-	107	87	72
Medium sand	67	80	94	64	51	40
Medium to coarse sand	74	94	-	72	57	42
Medium to very coarse sand	84	98-111	-	71	61	49
Medium sand to fine gravel	103	-	-	84	68	52
Medium sand to medium gravel	131	-	-	114	82	66
Medium sand to coarse gravel	164	-	-	134	108	82
Coarse sand	80	107	134	94	74	53
Coarse to very coarse sand	94	134	-	94	75	57
Coarse sand to fine gravel	116	136-156	-	107	88	68
Coarse sand to medium gravel	147	-	-	114	94	74
Coarse sand to coarse gravel	184	-	-	134	100	92

(1) Reduce by 10 percent if grains are subangular.

Figure 33. Standard Hydraulic Conductivities for sands based on degree of sorting and silt content (source: EPA, 1986 after Lappala, 1978).

Appendix D Groundwater Seepage and Flow

Table 12. Wells used to estimate flow through the aquitard and the values for Darcy's variables

KOH-0 well site	KOH-1 well	KOH-0 RWL (m below well collar)	KOH-1 RWL (m below well collar)	Aquitard thickness (m)	K aquitard (m/day)	Difference in Hydraulic (m)	Hydraulic gradient (m/m)	Cross sectional area of surface (m^2)
Oluwaya	WW201098	9.5	71	47	4.44E-08	61.50	1.309	1
Omboloka	WW201100	5.18	75	67	2.24E-08	69.82	1.042	1
Oshanashiwa	WW201102	16.04	77	59	4.44E-08	65.96	1.033	1
Ohameva	WW201104	10.62	71	76	4.44E-08	60.38	0.794	1
Epumbalo-ndyaba	WW201105	3.5	67	68	4.44E-08	63.50	0.934	1

Table 13. Amount of seepage through the aquitard layers

KOH 0 well	KOH 1 well	Q (cubic meters per sec)	Q (cubic meters per day)	Q (cubic meters per year)
Oluwaya (depression)	WW201098	5.82E-08	5.02E-03	1.83
Omboloka (Pan)	WW201100	2.33E-08	2.01E-03	0.735
Oshanashiwa (sand)	WW201102	4.97E-08	4.29E-03	1.57
Ohameva (depression)	WW201104	3.53E-08	3.05E-03	1.11
Epumbalondyaba(river)	WW201105	4.15E-08	3.59E-03	1.31

Table 14. Boreholes used to estimate horizontal flow within KOH-1 and the parameters for Darcy's variables

KOH 1 well	KOH 1 RWL (m below collar)	KOH 1 thickness (m)	T (m^2/day): after van Wyk (2009)	K (m/sec)	hydraulic gradient at site (m/m)	cross sectional area of flow (m^2)
WW201094	60	17	11	7.49E-06	6.6E-04	3.21E+06
WW201095	68	28	3	1.24E-06	6.6E-04	5.28E+06
WW201096	70	12	14	1.35E-05	3.1E-04	2.26E+06
WW201097	63	23	8	4.03E-06	3.1E-04	4.34E+06
WW201098	71	45	13	3.34E-06	8.4E-04	8.49E+06
WW201102	77	64	17	3.07E-06	1.4E-03	1.21E+07
WW201103	82	33	18	6.31E-06	3.5E-04	6.22E+06
WW201113	81	39	15	4.45E-06	4.4E-04	7.35E+06
WW201117	89	46	31	7.80E-06	2.8E-04	8.67E+06
WW201120	90	68	20	3.40E-06	5.1E-04	1.28E+07
WW201121	90	28	28	1.16E-05	1.9E-04	5.28E+06

Table 15. Estimated subsurface flow within KOH-1 at the given borehole sites

KOH 1 well	Q (cubic meters per sec)	Q (cubic meters per day)	Q (cubic meters per year)
WW201094	1.57E-02	1360	4.96E+05
WW201095	4.29E-03	371	1.35E+05
WW201096	9.38E-03	811	2.96E+05
WW201097	5.36E-03	463	1.69E+05

KOH 1 well	Q (cubic meters per sec)	Q (cubic meters per day)	Q (cubic meters per year)
WW201098	2.39E-02	2070	7.54E+05
WW201102	5.06E-02	4370	1.59E+06
WW201103	1.39E-02	1200	4.38E+05
WW201113	1.43E-02	1230	4.51E+05
WW201117	1.91E-02	1650	6.01E+05
WW201120	2.23E-02	1920	7.02E+05
WW201121	1.18E-02	1020	3.71E+05